DESIGN, DEVELOPMENT AND MANUFACTURING OF AN ALL TERRAIN MODULAR ROBOT PLATFORM

A THESIS SUBMITTED TO
THE GRADUATE SCHOOL OF NATURAL AND APPLIED SCIENCES
OF
MIDDLE EAST TECHNICAL UNIVERSITY

BY

MUSTAFA CİHANGİR KUL

IN PARTIAL FULFILLMENT OF THE REQUIREMENTS
FOR
THE DEGREE OF MASTER OF SCIENCE
IN
MECHANICAL ENGINEERING

MAY 2010

Approval of the thesis:

DESIGN, DEVELOPMENT AND MANUFACTURING OF AN ALL TERRAIN MODULAR ROBOT PLATFORM

Submitted by **MUSTAFA CİHANGİR KUL** in partial fulfillment of requirements for the degree of **Master of Science in Mechanical Engineering Department, Middle East Technical University** by,

Prof. Dr. Canan ÖZGEN _____
Dean, Graduate School of **Natural and Applied Sciences**

Prof. Dr. Suha ORAL (Chairperson) _____
Head of Department, **Mechanical Engineering**

Asst. Prof. Dr. A. Buğra KOKU _____
Supervisor, **Mechanical Engineering Dept., METU**

Asst. Prof. Dr. İlhan KONUKSEVEN _____
Co-Supervisor, **Mechanical Engineering Dept., METU**

Examining Committee Members

Prof. Dr. Y. Samim ÜNLÜSOY
Mechanical Engineering Dept., METU _____

Asst. Prof. Dr. A. Buğra KOKU
Mechanical Engineering Dept., METU _____

Asst. Prof. Dr. İlhan KONUKSEVEN
Mechanical Engineering Dept., METU _____

Asst. Prof. Dr. Yiğit YAZICIOĞLU
Mechanical Engineering Dept., METU _____

Assoc. Prof. Dr. Veysel Gazi
Electrical and Electronics Engineering Dept., TOBB ETU _____

Date: _____

I hereby declare that all information in this document has been obtained and presented in accordance with academic rules and ethical conduct. I also declare that, as required by these rules and conduct, I have fully cited and referenced all material and results that are not original to this work.

Name, Last name:

Signature:

ABSTRACT

DESIGN, DEVELOPMENT AND MANUFACTURING OF AN ALL TERRAIN MODULAR ROBOT PLATFORM

Kul, Mustafa Cihangir

M.S., Department of Mechanical Engineering

Supervisor: Asst. Prof. Dr. A. Buğra KOKU

Co-supervisor: Asst. Prof. Dr. İlhan KONUKSEVEN

MAY 2010, 80 pages

The aim of this thesis is to create a flexible multi-purpose modular all terrain robot platform, which has the potential to be used in commercial applications as well as in education and research. In developing this robot platform, it is aimed to use readily available commercial products as much as possible in order to keep the cost of the product low, increase maintainability, and benefit from the improvements made to these components in time. The modularity is attained by designing a two wheeled base module which is autonomous on its own. This base module is composed of two wheels where, the motors located inside these wheels. It is shown that the proposed base module facilitates the configuration of various robots to suit the needs of diverse applications. Detailed design and manufacturing of one of various possible configurations is presented. Performance tests are conducted on this robot configuration and effectiveness of the proposed modular approach is justified.

Keywords: Robot platform, all terrain mobile robot, modular robot, hub motor.

ÖZ

HER TÜRLÜ ARAZİ KOŞULUNDA GİDEBİLEN MODÜLER BİR ROBOT PLATFORMUNUN TASARIMI, GELİŞTİRİLMESİ VE ÜRETİMİ

Kul, Mustafa Cihangir
Yüksek Lisans, Makina Mühendisliği Bölümü
Danışman: Yrd. Doç. Dr. A. Buğra KOKU
Eş Danışman: Yrd. Doç. Dr. İlhan KONUKSEVEN

MAYIS 2010, 80 sayfa

Bu tezde ticari uygulamalarda olduğu kadar eğitim ve araştırmalarda da kullanılma potansiyeline sahip, esnek çok amaçlı ve her türlü arazi koşulunda hareket edebilen modüler bir robot platformu yaratılması amaçlanmaktadır. Bu robot platformunu geliştirilmesi sırasında, mümkün olduğunca fazla ticari ürünleri kullanarak, maliyetin düşük tutulması, bakım imkanlarının arttırılması ve kullanılan ticari parçalardaki iyileştirmelerden faydalanılması amaçlanmaktadır. Modülerlik, kendi başına da otonom olan iki tekerli temel bir modülün tasarlanmasıyla elde edilmiştir. Bu modül, içlerine motor gömülmüş olan iki tekerden oluşmaktadır. Önerilen temel modülün birçok farklı uygulamaya uygun çeşitli robot konfigürasyonlarına olanak sağladığı gösterilmiştir. Bu farklı robot konfigürasyonlarından bir tanesinin detay tasarımı ve üretimi sunulmuştur. Üretilen robot platformunun performans testleri yapılmış ve önerilen modüler yaklaşımın etkinliği ispat edilmiştir.

Anahtar kelimeler: Robot platformu, mobil robot, modüler robot, teker motor.

To My Family

ACKNOWLEDGEMENTS

The author wishes to express his heartfelt gratitude to his supervisor Asst. Prof. Dr. A. Buğra KOKU and his co-supervisor Asst. Prof. Dr. İlhan KONUKSEVEN for their excellent guidance, advices and encouragements throughout the thesis.

The author would like to thank his family, Şirin KUL, İsa KUL and Büşra KUL for their everlasting support, encouragement and patience throughout the research.

The author would also like to express his appreciation to Ulusal Kontrol Sistemleri Makina Tasarım SAN. ve TİC. LTD. ŞTİ. for their support during the research.

The support and cooperation of the author's colleagues and friends is gratefully acknowledged.

Master of Science Scholarship provided for the author by TÜBİTAK BİDEB, is gratefully acknowledged.

Finally, the author would like to thank his company TAI-TUSAŞ Inc. for letting of his thesis.

TABLE OF CONTENTS

LIST OF TABLES

TABLES

LIST OF FIGURES

FIGURES

LIST OF SYMBOLS AND ABBREVIATIONS

α	: Angle of the slope that the robot module is climbing up
a_{max}	: Maximum acceleration of the vehicle
A_r	: Minor diameter area of the screw
ATV	: All Terrain Vehicle
F_{air}	: Air resistance force
$F_{gradient}$	: Gradient resistance force
F_{mn}	: Normal force on the middle wheel
F_{mt}	: Maximum friction force on the middle wheel
f_r	: Coefficient of rolling resistance
F_{rn}	: Normal force on the rear wheel
$F_{rolling}$	: Rolling resistance force
F_{rt}	: Maximum friction force on the rear wheel
F_{total}	: Maximum estimated total force
$h_{obstacle}$	: Height of the obstacle
L	: Length between the centers of the wheels
M_m	: Total mass of a robot module
M_v	: Total mass of the robot platform
μ	: Coefficient of friction between tire and the surface
n_s	: Number of metric 3 screws used at rear cover
P_M	: Minimum required power output of the motor
θ	: Angle of the normal force on the middle wheel with lateral surface
τ_{screw}	: Shear stress acting on the metric 3 screws used at rear cover
W	: Vehicle tire load
V_{max}	: Determined maximum speed of the robot module

CHAPTER 1

INTRODUCTION

Reconnaissance, patrolling and exploration are the mission types among many that can be difficult or unsuitable for humans due to various reasons like, the hostility of the mission environment or inaccessibility to this environment. As a solution to accomplish these missions, mobile robots come into view. In today's world robots in various sizes and shapes are being used in diverse environments from exploration of the other worlds to the military applications on the battlefield. For the robots aspects like adaptability to different environments becomes important, when parameters like cost and maintenance are considered.

The cost, maintenance and availability of the current products in the market make it hard to access for public. Also the products are generally a built with a narrow mission range. For these reasons in order to provide a feasible robot platform, in terms of cost and easiness of use, for the researchers, it is aimed to create a multipurpose, modular, all terrain mobile robot platform by using the readily available commercial products as much as possible.

As stated at the beginning robot platforms can be in various sizes. These platforms can be divided into four empirical categories with respect to their dimensions, namely large, medium, small and mini. Each of these categories has their own advantages and disadvantages.

The first category, which is named as large, consists of platforms at size of a car or a truck. An example to this category can be given as Crusher robot, which is shown in Figure 1. It is created by Carnegie Melon University as a part of a project that is

funded by DARPA. Its length is just over 5 meters and its width is about 2.6 meters. A turbo diesel engine is used as generator to charge the batteries which are providing energy to the electric hub motors [1]. This robot type can traverse long distances and has a high payload carrying capacity which makes it suitable for missions like patrolling and supply support, but it is not very suitable for search missions due to its large size which makes the travel at environments like forest impossible and its high cost which makes it difficult to use several robots.

Figure 1 Crusher robot travelling at rough terrain [1]

The second category, which is stated as medium, consists of platforms that has a size smaller than the first category but still cannot be carried by humans. An example to this category can be given as İzci developed by Aselsan, which is shown in Figure 2. The robot platform base is a modified ATV. The main mission objective of this robot is border patrolling. Again its relatively large size makes it possible to carry high enough energy reserves to enable long mission times and with its relatively high speed wide working area but its size becomes a disadvantage which makes it unsuitable to use this robot type at environments like forests and caves where the platform cannot travel.

Figure 2 İzci robot developed by Aselsan [2]

The third category, which is stated as small previously, consists of robot platforms that can be carried by humans. There are several commercial examples of this type of robots, like Packbot or Pioneer. This type has a wide range of applications from education to military. Their relatively low cost with respect to the bigger robot types makes it affordable to use several robots at the same time. Their size gives them the advantage of travel in terrains where bigger vehicles cannot operate. Their size is at the same time disadvantageous in terms of load carrying capacity and working time without replenishing the onboard energy source.

The final category stated previously, namely mini category, are the platforms where the size of the robot usually can fit to one's hand. This robot type is generally used in swarm robotics. Main principle in using this type is to solve problems by cooperation of the several same kind of robot when a single robot cannot achieve this goal on their own. The size limits the load carrying capacity the onboard energy source which is important in terms of mission range. For this reason the capabilities of this kind of robots is generally lower than the other size classes.

When robot capabilities of each category are compared with each other, it is observed that with the smaller size, movement capability at the narrow environments increase. The cost of this gain is loss of working time capacity and the decrease in the range of the pay load carrying capacity. It is decided to create the flexible robot platform in small size factor as a compromise between the payload carrying capacity and mobility.

The survey during the determination of the size factor showed the confirmation of the importance of adaptability and cost. The survey revealed one of the problems of the well known example platforms for the researchers, which is their affordability. Even a single robot platform can cost tens of thousands dollars, let alone a group of robots which the user might need in different mission types which brings another issue that is targeted at this thesis modularity. Although many robot platforms in the market considered as modular, their capabilities fall short of the modularity concept of this thesis; since modularity in these robot platforms is generally regarded only as the ability to change the payloads on a main body with respect to the mission. However, the modularity concept, in the context of the thesis, is defined as the user's ability to change the size and shape of the robot main body and the locomotion system along with the payload to suit the needs of different applications. This can even lead to situations where the robot platform itself becomes a payload used to give movement ability to otherwise inanimate large platforms. After these arguments, the motivation of this thesis can be claimed as to create a modular robot platform to fill the needs of researchers, or other users, of a robot platform which has a wide application area at an affordable price.

In the scope of this thesis a robot platform with the properties of modifiable main body size and locomotion type is designed. In order to achieve this goal electric motor and gear head are moved out of the main body. Several example robot platform configurations, with the capabilities like ability to move even in the case of turning upside down, are described; and the detail design of the most feasible platform is realized and manufactured. Also a conceptual suspension system is designed in order the robot platform to handle the rough terrain better. Tests on the

manufactured platform are performed in order to see whether or not the determined platform meets the specifications that are determined based on the literature survey.

The outline of the following chapters can be summarized as follows. In the next chapter, “literature survey” is presented where; several examples of robot platforms in the small form factor category are examined. After the examination of the robots, in chapter 3 “robot platform configuration and design parameters”, the robot platform specifications are determined based on the specifications of the robots found on the literature survey and several different conceptual design configurations are described. Using the specifications determined at the third chapter, in chapter 4 “detailed robot platform design”, as the name implies detailed design of the robot platform is described. The performance of the robot in the real world is tested and discussed in the chapter 5 “test environment and results”. And in the last chapter, chapter 6 “conclusion and future work”, what is done throughout the thesis and can be done after the thesis on this project is discussed.

CHAPTER 2

LITERATURE SURVEY

In this chapter the results of conducted literature survey are inspected. Survey is based on the determined robot base size factor stated at the introduction which revealed platforms with missions ranging from military to education and research. Several example platforms, found at the survey, are analyzed in terms of their size, weight, speed and other attributes.

The first platform that is analyzed is the Talon robot platform which is shown in Figure 3. Talon is a tracked multipurpose military robot developed by Foster-Miller Inc., with application areas such as reconnaissance and combat. The robot is remote controlled and it can carry 45kg of payload for different mission types. Robot itself weighs 52 to 71 kg and its dimensions are 86.4cm by 57.2cm by 42.7cm (height when the arm of the robot is stowed). The maximum speed of the Talon is 2.3m/s. It can climb $45°$ slopes. The on board batteries provide a 2.8 hours of operation time without charging also additional batteries can be added as an option [3]. A bare Talon robot platform cost about $60,000 [4].

The second platform that is analyzed is Chaos robot (Figure 4). The robot is a product of Autonomous Solutions Inc. and cost more than $120,000. The locomotion system of the robot is a hybrid track and arm system. The four arm of the robot that can move independently, is tracked. The robot is teleoperated, there are built in algorithms that is assisting the user while driving the robot. The maximum speed of the robot is about 2.2m/s. It can climb $45°$ slopes. The weight of the robot is 55kg and its dimensions are 71cm (with retracted arms) by 68.5cm by 20cm (with flat arms). The robot can carry different payloads for different operations. The operation time of Chaos robot without charging is 2 hours [6].

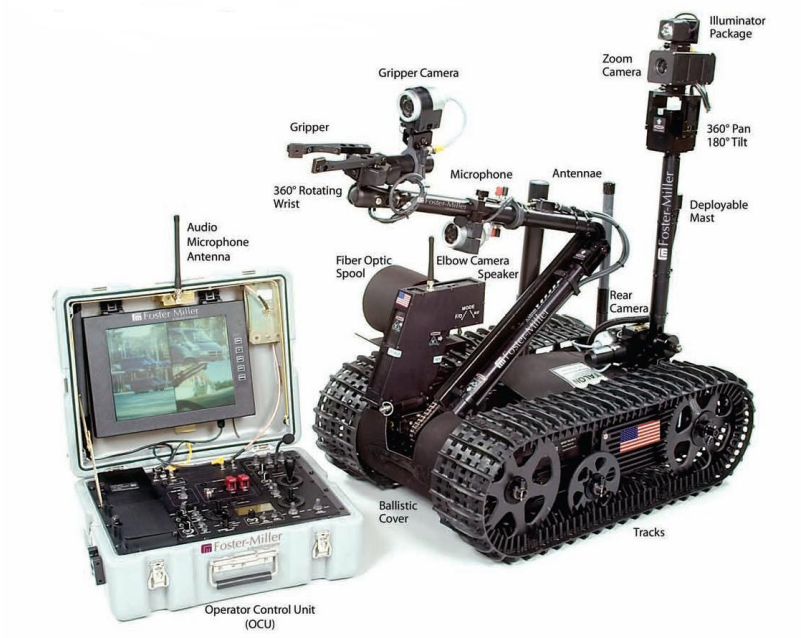

Figure 3 Talon robot and its operator controller unit [3]

Figure 4 Chaos Robot going over rubble [5]

The next example robot platform that is analyzed is the product of Mesa Robotics, the Matilda robot (Figure 5) which cost around $25,000. Matilda is a tracked robot platform. The robot has a maximum speed around 0.9m/s. It can climb up to $50°$. The robot is remote controlled. The weight of the robot is around 27.7kg and its dimensions are 76.2cm by 53.3cm by 30.5cm. Matilda can carry 56.7kg of payload. According to its specifications this robot platform has an operation time of 6 to 10 hours [7].

Figure 5 Matilda robot [7]

Another worth to mention robot platform is Packbot (Figure 6). Packbot is developed by iRobot Corporation and has a cost around $40,000. It has different types of kits for different types of missions. Packbot can reach speeds up to 2.6m/s and it can climb up to %60 grade ($30°$) slopes [9]. The robot is remote controlled. The weight of the robot is 19.1kg and its dimensions, with flippers stowed, are 69.9cm by 52.1cm by 19.1cm. Packbot can carry up to 20.9kg of payload. The onboard batteries supply enough power for 2 to 12 hours of operation time (depending on the mission) without recharging [8].

Figure 6 Packbot with mapping kit [8]

The inspected robots up to this point are tracked robots. From this point on examples of wheeled robot platforms are analyzed. The first wheeled mobile robot among small sized robots survey is Pioneer 3-AT robot (Figure 7), which at a cost of $4,000. The robot is developed by Mobile Robots Inc.. The locomotion system consists of four wheel differential drive. The robot can reach speeds up to 1.2m/s and can climb up to %35 grade (19°) slopes. Pioneer has a weight of 12kg and has a payload capacity of 20kg, on concrete surface. Its dimensions are 50cm by 49cm by 26cm. The on board battery provide enough energy to sustain 4 to 8 hours of operation time without recharging [11].

Figure 7 Pioneer 3-AT robot [10]

Another popular wheeled robot platform is the Koala II (Figure 8). The robot is developed by the K-TEAM Corporation. The maximum speed of the robot is 0.6m/s. The robot can climb up to 43° . Robot base weight is 4kg with the batteries. Readily available expansion modules as well as custom built accessories can be mounted to the robot and maximum payload carrying capacity is 3kg. Robot dimensions are 32cm by 32cm by 20cm. The robot can operate approximately 4 hours without out recharging when the robot is carrying its maximum payload capacity [12].

Another robot that will be included in this survey is Gaia-2 robot (Figure 9). The robot is a product of AAI Canada Inc.. The maximum speed of the robot is 0.8m/s. The weight of the robot is 40kg and it has a load carrying capacity of 20kg. The dimensions of the robot are 49cm by 53cm by 26.5cm. It can go over 15cm high obstacles. The operation time of the robot without needing recharge is 5 hours [13].

Figure 8 Koala II robot [12]

Figure 9 Gaia-2 robot [13]

The last robot that is analyzed in this survey as an example is the MMP-8 mobile robot platform (Figure 10) produced by The Machine Lab Inc.. The maximum speed of the robot is around 1.1m/s. The robot is operated with remote control. The weight

of the robot is around 3.4kg and it has a load carrying capacity of around 3.2kg. The dimensions of the robot are around 38.7cm by 31.8cm by 10.8cm. The operation time of the robot with one charge is around 45 minutes with the onboard battery. One important feature of this robot is that it the two halves of its body can rotate with respect to each other and it has a passive suspension system between these two halves of the body [14]. The price of the robot is $795 [15].

Figure 10 MMP-8 robot platform [14]

The comparison of the example robot platforms is shown in Table 1. The “-” sign at some cells of the table mean information related to the specification of the robot platform couldn’t be found during the literature survey. Some of the properties of the examples vary greatly, such as the maximum speed and the payload carrying capacity properties. The maximum speed of the examples is ranging from 0.6m/s to 2.6m/s. The payload carrying capacity of the examples is changing from 3.2kg to

56.7kg. Further discussions about the specifications of the example robots are carried on at the next chapter.

Table 1 Comparison table of the example robot platforms

ROBOT	Dimensions (cm)	weight (kg)	payload capacity (kg)	speed (m/s)	Max. slope robot can climb (°)	Operation time with one charge	Suitable for autonomous robotics research
Talon	86.4x57.2x42.7	51 to 72	45	2.3	45	2.8 hours	No
Chaos	71x68.5x20	55	-	2.2	45	2 hours	No
Matilda	76.2x53.3x30.5	27.7	56.7	0.9	50	6 to 10 hours	No
Packbot	69.9x52.1x19.1	19.1	20.9	2.6	30	2 to 12 hours	No
Pioneer 3-AT	50x49x26	12	20	1.2	19	4 to 8 hours	Yes
Koala II	32x32x20	4	3	0.6	43	4 hours	Yes
Gaia 2	49x53x26.5	40	20	0.8	-	5 hours	Yes
MMP-8	38.7x31.8x10.8	3.4	3.2	1.1	-	45 minutes	Yes

Apart from these platforms there are two other platforms that worth to mention due to their unique designs. The first one is a robot platform that is created by Gökhan Bayar in his thesis, which can be seen at Figure 11. This robot platform can reach up to speeds of 0.9 m/s and can climb slopes up to 43°. The dimensions of the robot platform are 30 cm by 45 cm by 20 cm and it can carry 10kg of payload. The robot can operate without recharging about 2-3 hours [16]. The importance of this Platform is that the commotion system can be changed from tracks to wheels easily.

The second robot platform is Galileo robot platform which can be seen at Figure 12. The importance of this robot platform is its unique locomotion system. The robot can

be described as a two wheeled platform but there is a unique mechanism inside the wheels. When the mechanism is activated the retracted arms inside the wheels opens and they stretch the rubber around the wheel and use the rubber as a palette thus effectively turning the locomotion system to tracked platform [17].

Figure 11 Robot platform created by Gökhan Bayar [16]

Figure 12 Galileo robot [18]

To sum up although example robot platforms so far observed during the literature survey can carry different kinds of payload with respect to the different missions and even can change its locomotion type, they cannot be qualified as truly modular in

the context of this thesis due to their lack of ability to have a flexible design capacity for the size and shape of their bodies which is one of the goals of the robot platform described in this thesis.

CHAPTER 3

ROBOT PLATFORM CONFIGURATION AND DESIGN PARAMETERS

In this chapter, the general specifications of the aimed robot platform is determined based on the discussions about the example robot platform specifications such as speed and payload carrying capacity in order to create a configuration that can compete with the other commercial products in the market. In the scope of the thesis possible design configurations of the robot platform are discussed and detailed design of one of the possible configurations is performed at the next chapter.

The first design specification parameter that is discussed is the maximum slope degree which the robot platform can climb. Specifications at the Table 1 show that apart from the two of the robot platforms, the example robot platforms can climb around 45°. For this reason it is determined to design the robot platform with the ability to climb 45°.

The second design parameter that is discussed is the locomotion of the robot platform which can be dived to two parts, first part is locomotion type and second part is speed. For the locomotion type tracked and wheeled type platforms are examined in the literature survey, and considered as the viable alternatives for the robot platform. Both of these systems have advantages and disadvantages over each other. For example tracked platforms can handle better rough terrains but if something stuck in their tracks they can lose their mobility whereas multi wheeled platforms might be able to move even if they lost one of the wheels. For this reason best locomotion solution is an interchangeable design where the user can change wheels with tracks easily. With the proposed design concept, even omniwheels can be used which can be considered as a special case of wheeled design, turning the robot to a holonomic platform. When the example robots in the literature survey are

examined for the second part of the locomotion design parameter, it is observed that apart from three of the robot platforms the speed of the example robots is around 0.6-1.2m/s. For this reason it is determined to choose a suitable motor and gearbox pair to the robot platform which can satisfy a maximum speed in the 0.6-1.2m/s range, along with the maximum climbable slope requirement.

The third design parameter that is discussed is the main body and payload carrying capacity of the robot platform. When the example robot platforms are investigated, although the example robots are regarded as modular platforms it is observed that their fixed main bodies is a hindrance in achieving the different possible configurations. It is also determined, from observation of example platforms, that the motor with drive train becomes a limiting factor in the main robot body design when they are inside the main body. Also when the motor and the drive train are inside the main body, they reduce the available volume inside the main robot body for the payload. For these reasons, motor and the other elements of the drive train are decided to be placed to the area inside the locomotion system. Also in order to increase the flexibility it is decided to create the robot platform from modules.

For the wheeled design type modular platform, each module is determined to have at least two wheels since the minimum required number of wheels for a differential drive is two. Since it is determined to place the motor and the gearbox into the wheel the dimensions of the main body can be chosen such that the body stays inside the wheel dimensions. This configuration gives advantage of ability to move even in the case of tip over.

The simplest robot configuration is a two wheeled differential drive platform, which is illustrated in Figure 13. The stability of the robot platform can be maintained by using internal balancing systems or simply mounting caster wheel to the front and back of the robot platform. This platform is referred as robot module from this point on. The robot modules are used as the building block of the more complex robot configurations which is described in remaining part of the chapter. The total mass of a single module is determined as seven kilograms, with a payload to total mass ratio

around %40 in order to have a comparable load carrying capacity with the example robot platforms in the literature survey.

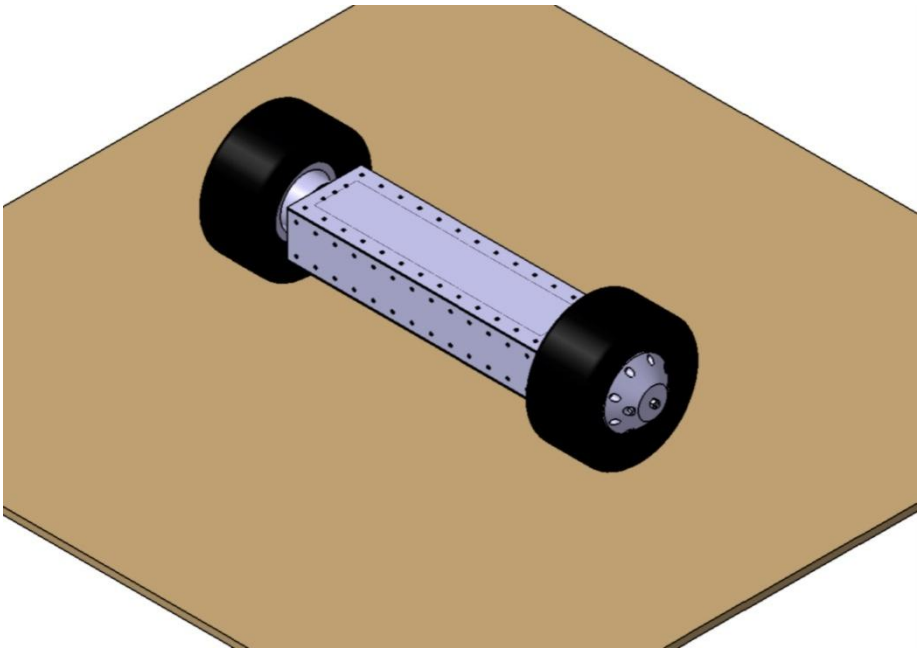

Figure 13 Robot Module: a two wheeled robot platform

The capability of a single module is limited. For this reason in order to have increased capability a new robot platform is created by connecting modules together. One connection type is rigid connection of the n many modules. An example platform formed by connecting three modules is illustrated in Figure 14. Of course there are several variations of rigid connection configuration. For example the modules can be connected with connectors of unequal length (Figure 15) or extra payload bays can be attached to the connectors which are represented with grey boxes at Figure 16. Also a suspension system that works even if the robot tips over can be added to the modules in order to reduce the vibrations during traversing on rough terrain. A representation of this system is illustrated in Figure 17.

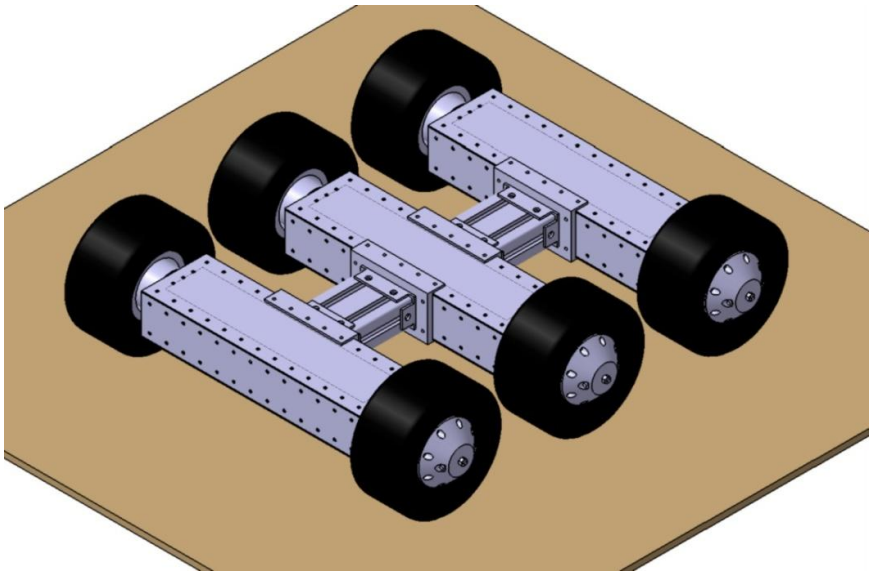

Figure 14 A Robot platform created by rigid connection of three modules

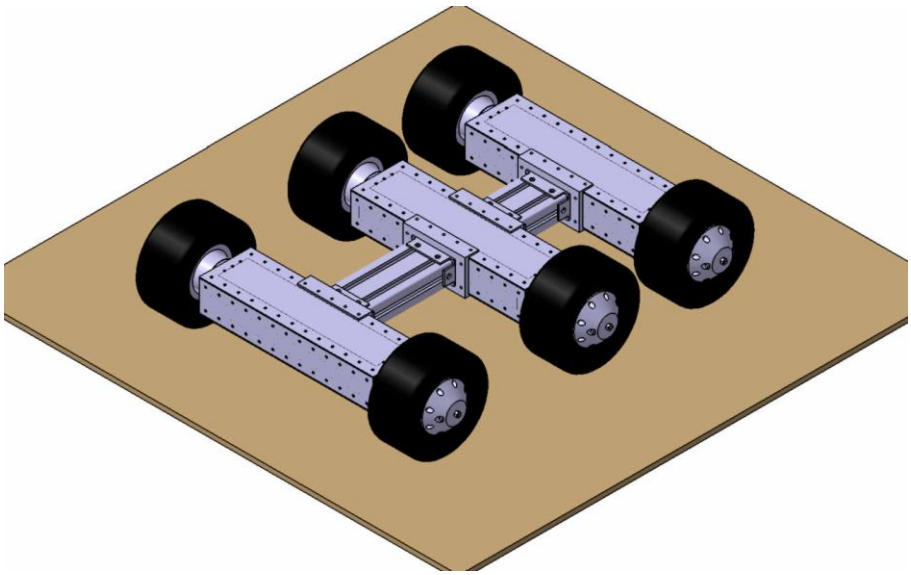

Figure 15 Three module robot platform with asymmetric connection length

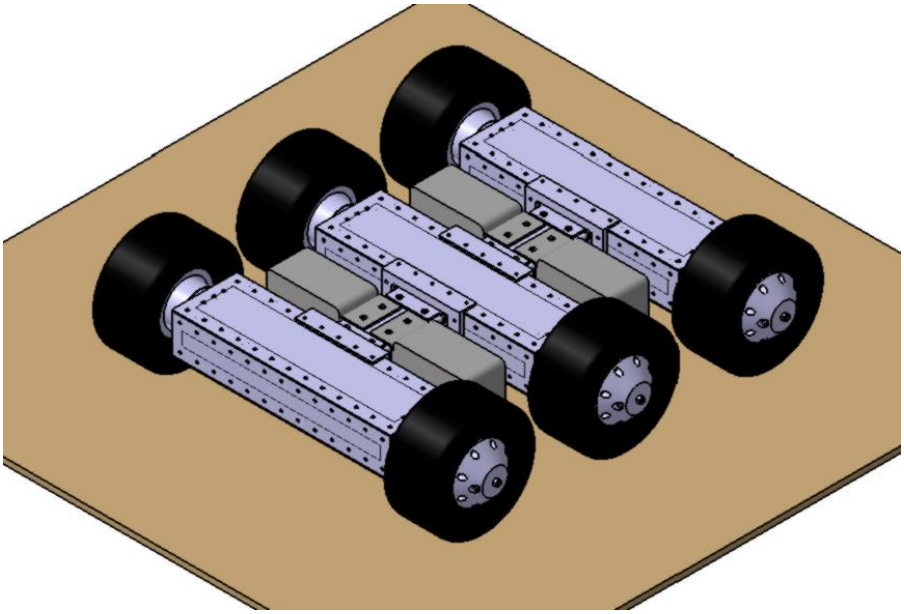

Figure 16 Three module robot platform with extra load bays

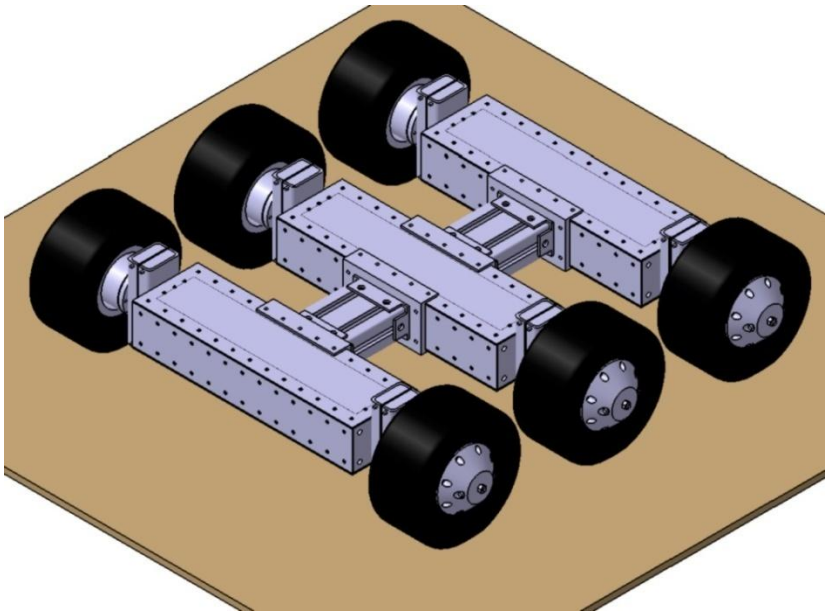

Figure 17 A representation of the three module robot platform with suspension

The connections between the modules don't always have to be rigid; also the module itself doesn't have to be in rectangular prism shape. An example 2 module platform with a revolute joint between the modules is illustrated in Figure 18. The joint, which can be seen as the yellow part at the Figure 18, in the example helps to keep all the wheels connected to the ground while going over rough terrain by adding an additional degree of freedom in roll axis.

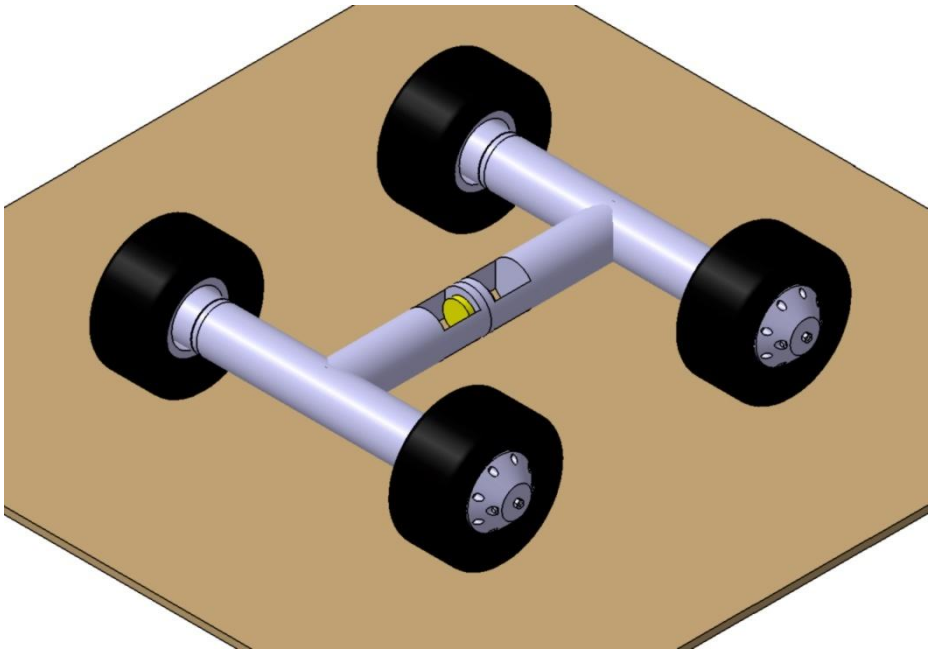

Figure 18 Two module platform with revolute joint

The degree of freedom of the previous example platform can be increased by adding new revolute joints near to the modules. The model is illustrated in Figure 19. The new joints give the modules the ability to turn in yaw axis with respect to each other. This unique arrangement, gives the robot platform steering ability similar to the fifth wheel steering instead of a differential drive style.

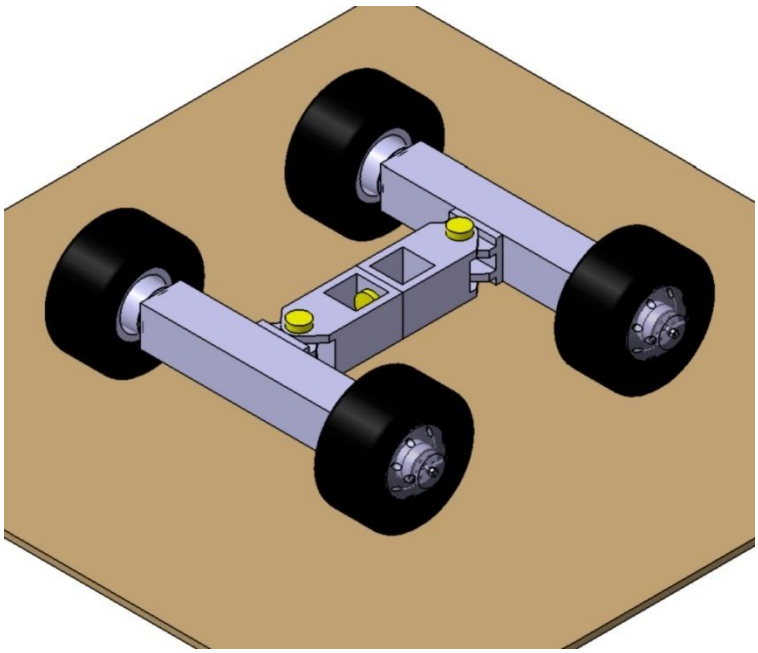

Figure 19 Two module robot platform with increased degree of freedom

As stated before, this proposed modular system can be turned into a tracked robot platform. The platform locomotion system grants this by an easily retractable tire and rim assembly. The tire and rim is replaced with a track pulley at this configuration. An example tracked platform is illustrated in Figure 20.

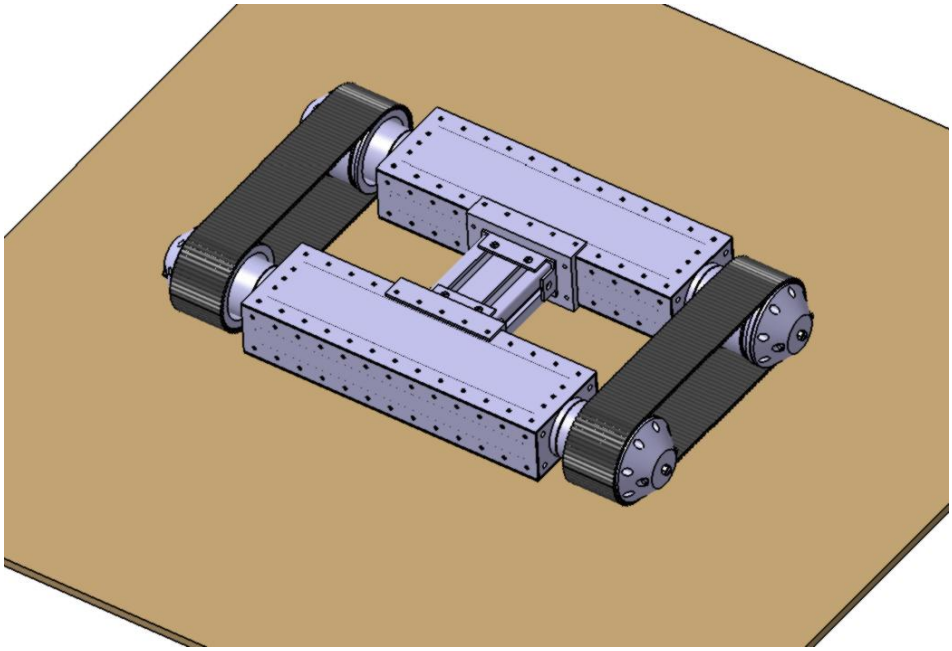

Figure 20 Tracked robot platform formed by using two modules

In this chapter based on the example robot platform specifications in the literature survey, the specifications of the designed robot platform are determined be as follows: The speed of the platform is in the range of 0.6 to 1.2m/s. Robot platform is to climb up a 45° slope. Robot platform has a maximum 2.8kg payload carrying capacity per module. In order to show the plausibility of the robot platform design, among many stated conceptual configurations, it is determined to create the detail design of the robot platform shown in Figure 14 due to its relative simplicity. The designed robot platform is then manufactured and tests are performed in order to check the determined requirements are whether satisfied or not.

CHAPTER 4

DETAILED ROBOT PLATFORM DESIGN

In this chapter details of the example conceptual model are inspected. First minimum power required for this robot platform is calculated by using this value an appropriate motor, gear box and battery is selected, and then detailed design of the wheel motor system and main body is presented after that a novel suspension system for the robot platform is described and finally the control system of the robot platform is introduced.

4.1. Power Requirement Calculations

For calculation of the minimum required power, maximum estimated total force and the maximum desired speed must be known. The maximum estimated total force is equal to the sum of gradient resistance force, air drag force (which can be assumed as zero), rolling resistance force and inertial force, which is equal to mass times acceleration.

$$F_{total} = F_{gradient} + F_{air} + F_{rolling} + M_m \times a_{max} \quad (4.1)$$

Where:

F_{total} : Maximum estimated total force

$F_{gradient}$: Gradient resistance force

F_{air} : Air resistance force

$F_{rolling}$: Rolling resistance force

M_m : Total mass of a robot module

a_{max} : Maximum acceleration of the vehicle

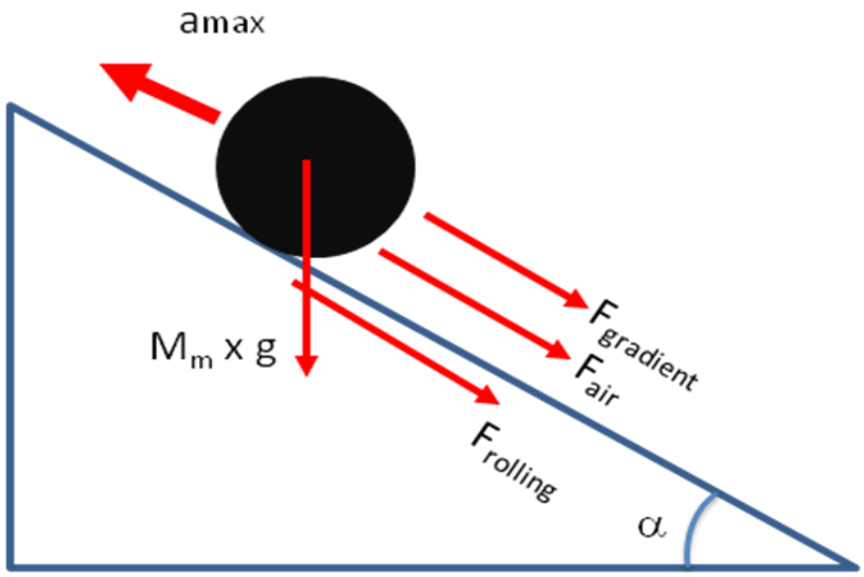

Figure 21 Forces acting on the Robot module

The maximum total force calculation is performed for a single robot module. The forces acting on the robot module is shown in Figure 21. Calculations regarding these forces can be seen at below.

The first component that is calculated is the Gradient resistance force. Gradient resistance force is the component of the weight of the module that is parallel to the road. Maximum gradient force occurs when the robot module climbs a slope with the maximum designated angle which is determined as 45° at the chapter 3. The formula of the gradient resistance is:

$$F_{gradient} = M_m \times \sin\alpha \times g \quad (4.2)$$

Where:

α : Angle of the slope that the robot module is climbing up

The result of the (4.2) for 7 kilograms of estimated robot module mass and $45°$ slope is:

$$F_{gradient} = M_m \times \sin\alpha \times g = 7 \times \sin 45° \times 9.81 \cong 48.56\ N \quad (4.3)$$

The third component, rolling resistance occurs mainly due to the deformation on the road and the tire surfaces and it can be calculated with the formula below:

$$F_{rolling} = f_r \times W \quad (4.4)$$

$$W = M_m \times \cos\alpha \times g \quad (4.5)$$

Where:

f_r : Coefficient of rolling resistance

W : Vehicle tire load

Maximum estimated total force is assumed to be occurring at robot moving on a slope with unmaintained natural road conditions. For this reason is chosen as 0.16 from Table 2. By using this at formula (4.4) for a robot module with 7kg mass, the estimated rolling resistance is calculated as:

$$F_{rolling} = f_r \times W = f_r \times M_m \times \cos\alpha \times g = 0.16 \times 7 \times \cos 45° \times 9.81 \cong 7.77\ N \quad (4.6)$$

Table 2 Estimated coefficient of rolling resistance table [19]

Road Surface	f_r
Very good concrete	0.008-0.010
Average concrete	0.010-0.015
Concrete in poor condition	0.020
Very good tarmac	0.010-0.0125
Average tarmac	0.018
Tarmac in poor condition	0.023
Very good macadam	0.013-0.016
Average macadam	0.018-0.023
Dusty macadam	0.023-0.028
Good Stone paving	0.033-0.055
Stone paving in poor condition	0.033-0.055
Snow(50mm layer)	0.025
Snow(100mm layer)	0.037
Unmaintained natural road	0.080-0.160
Sand	0.150-0.300

The last component of the estimated total force comes from the acceleration. It is assumed that the robot has an acceleration of 0.5 m/s^2 at the maximum power need conditions. The estimated maximum total force can be found when the results of the equations (4.3), (4.6) and the maximum acceleration and determined mass of the module are put into the equation (4.1).

$$F_{total} = F_{gradient} + F_{air} + F_{rolling} + M_m \times a_{max} = 48.56 + 0 + 7.77 + 7 \times 0.5$$

$$F_{total} = 59.83\ N \tag{4.7}$$

After the calculation of the maximum total force, minimum required power output of the motor can be calculated by multiplying the maximum total force with the desired maximum operational speed. From here the power is calculated as:

$$P_M = F_{total} \times V_{max} \tag{4.8}$$

Where:

P_M : Minimum required power output of the motor

V_{max} : Determined maximum speed of the robot module

As stated at the chapter 3, maximum desired speed for the module is determined to be in the range of 0.6 to 1.2 m/s. For this calculation maximum speed is assumed to be 1.2 m/s. By putting the values of the variables of equation (4.8) minimum required power is found as:

$$P_M = F_{total} \times V_{max} = 59.83 \times 1.2 = 71.80W \tag{4.9}$$

It should be noted that calculated minimum estimated power requirement is for two wheeled robot module the power requirement of a single wheel is 35.90 W. When criteria such as procurement time, size, power output, price and after market are taken into consideration, brushless RC plane motor Aoxing 18 ax 3020 800kv Brushless is selected among the other candidates. However it should be noted that the maximum climbable slope is also related to the coefficient of friction between the surfaces. For this reason even if there is enough motor power, robot platform might not be able to climb the desired slope.

The assumed power source for the gearbox selection that is used in this system is four cell lithium polymer battery with a 14.8 output voltage. For this voltage level estimated current usage at the maximum power need is around 2 A. For an operation time of around 1.5 hours and suitable dimensions, a lithium polymer battery with 3400mAh capacity is chosen as power source per wheel.

The voltage output of the selected battery creates an 11,840 rpm motor speed. In order to lower this value to rotational speeds around 2 rps, which gives the ability of 1.1m/s travel speed to robot platform for a 0.170m diameter tire which is commonly used at the RC cars, a gearbox with a reduction ratio around 1:80 to 1:100 is needed. Upon market research, aftermarket gearbox of Einhell brand electric hand screw driver, which has a 1:81 gear ratio, is selected with respect to the parameters like price, availability and dimensions. The resulting maximum velocity with this motor and gear set becomes 1.3m/s.

4.2. Wheel and Main Body Design

Before starting the wheel and main body design, estimated maximum force at the worst case scenario is calculated.

For design check calculations the worst case scenario in terms of forces acting on the base is determined as the fall from one meter to the ground at the initial deployment of the robot platform. The behavior of the tires can be modeled as combination of spring and damper, so the system can be assumed to be a mass, spring, damper system. Two assumptions are made for the modeled system.

- The damping of the tires is neglected, thus the system model reduced to a spring mass model. Since some of the kinetic energy is absorbed by the damping of the tires neglecting it during maximum force calculations will result in higher than real life which make the design check more conservative.

- The spring constant is assumed to be not changing with respect to the deflection of the tire under the applied load.

After these assumptions the two wheeled module fall can be modeled as in Figure 22 below.

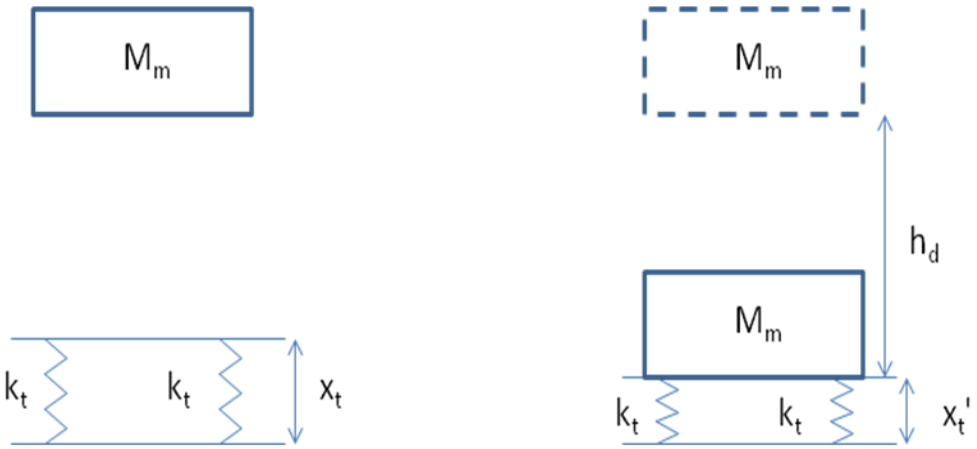

Figure 22 The model of the module before (left side) and after (right side) the fall

where

M_{mr} : Estimated mass of the module (without the rubber tire)
k_t : Spring constant of the rubber tire
x_t : Distance of the rubber tire center from ground before deflection
x_t' : Distance of the rubber tire center from ground at the maximum deflection
h_d : Desired module fall height

The maximum force calculation is based on the conservation of energy principle. All the potential energy of the module will be stored at the tire, which is assumed to be acting as a spring, after the fall. The energy conservation formula of this event can be found at below.

$$\frac{1}{2} \times (k_t + k_t) \times (x_t - x_t')^2 = M_m \times g \times h_d \quad (4.10)$$

When the equation is rearranged and necessary cancellations are done maximum deflection $(x_t - x_t')$ can be written as below.

$$(x_t - x_t') = \sqrt{\frac{M_m \times g \times h_d}{k_t}} \tag{4.11}$$

The maximum force form the tire can be found with the formula below.

$$F_{tmax} = k_t \times (x_t - x_t') \tag{4.12}$$

When $(x_t - x_t')$ is replaced with its equivalence from the (4.11) the above formula becomes:

$$F_{tmax} = k_t \times \sqrt{\frac{M_m \times g \times h_d}{k_t}} \tag{4.13}$$

After the simplification of (4.13) F_{tmax} is:

$$F_{tmax} = \sqrt{M_m \times g \times h_d \times k_t} \tag{4.14}$$

The gravitational acceleration constant and the estimated mass and module fall height can be seen below.

$M_m = 7\ kg$

$h_d = 1\ m$

$g = 9.81 \frac{m}{s^2}$

In order to determine the stiffness of the tire a test is conducted. Test platform is shown in Figure 23. As can be seen from Figure 23, the two tires are equally loaded via a rod and the deflections of the tires are measured from the white extruded bar

on the top of the wheels with respect to the block stationed on the platform by using a caliper. The average of displacement at both sides is calculated and used to create the Figure 24. From test data, which is shown in Figure 24, the spring constant of the two combined tires is 22,239N/m and from here stiffness of one tire is determined as 11,119.5 N/m.

Figure 23 Wheel stiffness measurement test platform

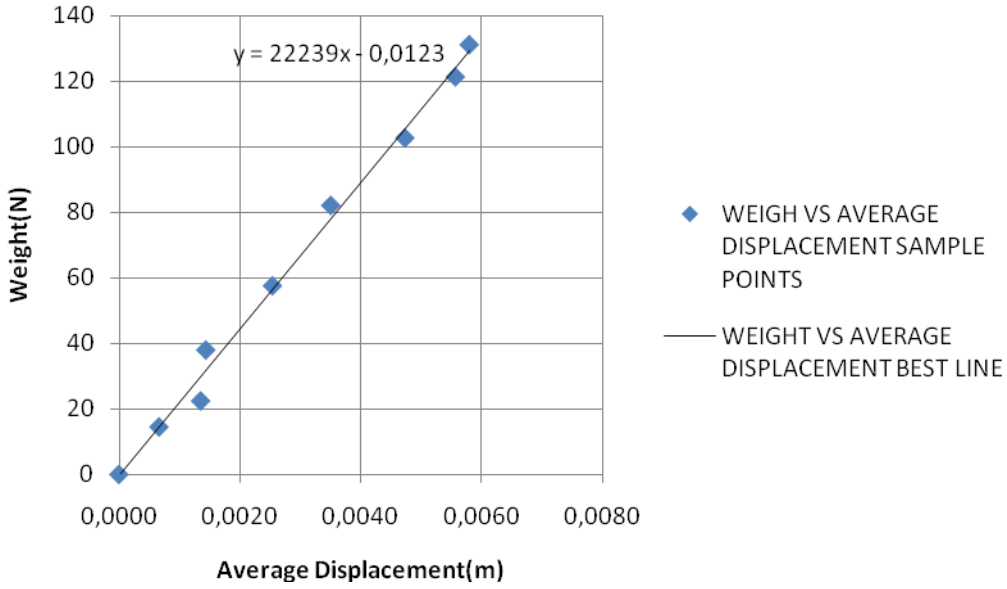

Figure 24 Applied Weight vs. Average Displacement of Two Tires graph

When these values are put into equation calculated F_{tmax} is:

$$F_{tmax} = \sqrt{\mathrm{M_m} \times \mathrm{g} \times \mathrm{h_d} \times \mathrm{k_t}} = \sqrt{7 \times 9.81 \times 1 \times 11119.5} \cong 873.83\ N \qquad (4.15)$$

Although estimated maximum force is calculated, it should be noted that the real world values are lower than the calculated value since the energy losses due to damping is not taken into account during the calculations, as stated before.

Based on, result of the estimated maximum force calculation (4.15) and the chosen motor gearbox pair, a wheel with the hub motor is designed which is shown in Figure 25.

Figure 25 Solid model of the new designed wheel

The wheel consists of an inner body, where the motor and the gearbox are housed, and a two part rim. The exploded view of the wheel is shown in Figure26. The names of the parts which are indicated with the numbers at the exploded view can be seen at the Table 3. Important Items are described at the following part of the section.

Table 3 Names of the detail wheel parts

WHEEL PART LIST			
1	Tire	14	Gearbox front holder
2	Cable holder	15	Output shaft of gearbox
3	Rear cover	16	Output shaft holder
4	Rear Cover Seal	17	Plain bearing
5	Motor	18	İnner hub case
6	Motor holder	19	Bearing
7	Coupling	20	Bearing holder
8	Gearbox Rear holder	21	Rim primary part
9	Gearbox Rear Protector	22	Rim seal
10	Input Sun Gear	23	M3 nut
11	Planet Gear block	24	M3 bolt
12	Pin	25	M5 nut
13	Ring gear	26	Rim secondary part

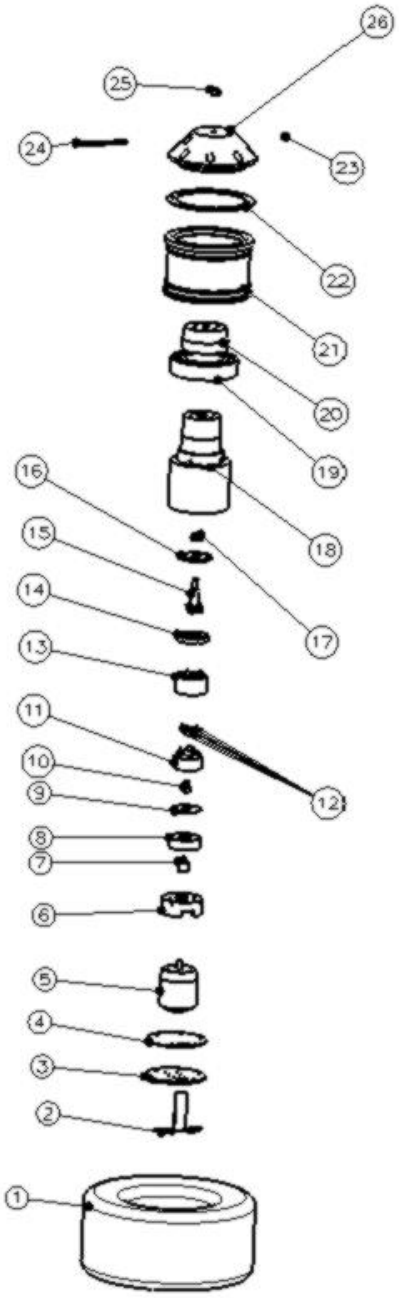

Figure 26 Exploded view of the wheel

Tire, which is the first one of the labeled parts at the exploded view, is selected as a foam filled rubber tire which are used at 1/8 scale off road RC cars. The tire has a diameter of 0.17m and a thickness of 0.08m.

The item labeled as number two at the Figure 26 is cable holder. It is used to prevent the cables of the outrunner brushless motor to touch the motor itself. Also the Hall Effect sensor used for motor speed measurement is attached to this part. Detailed drawing of the part can be found at Appendix A.

Item number three, the rear cover, which is shown in Figure 27, works both as a connection base to the main robot body and the inner hub case. Technical drawing of the part can be found at the Appendix A. Six metric 3 screws are used at the inner hub case connection and metric 4 screws are used at the main body connection. The most critical part of this item, in fact the most critical part of the wheel assembly, is determined as the shear stress caused by the estimated maximum force on the six metric 3 screws. The shear stress on the screws can be calculated as:

$$\tau_{screw} = \frac{F_{tmax}}{n_s \times A_r} \tag{4.16}$$

Where:

τ_{screw} : Shear stress acting on the metric 3 screws used at rear cover

n_s : Number of metric 3 screws used at rear cover.

A_r : Minor diameter area of the screw

As stated before number of metric 3 screws used at rear cover installation is 6 and the minimum area is 4.47mm^2. Using the maximum estimated force, which is found at (4.16), the shear stress of a screw is found as:

$$\tau_{screw} = \frac{F_{tmax}}{n_s \times A_r} = \frac{873.83}{6 \times 4.47 \times 10^{-6}} = 325812826\ Pa \cong 32.58\ MPa \tag{4.17}$$

The shear stress acting on the screw is 32.58 MPa. With respect to the maximum shear stress theory, the factor of safety, which is ratio of the shear stress acting on the steel screw to the half of the yield strength of the steel screw (170MPa), is found as 2.6.

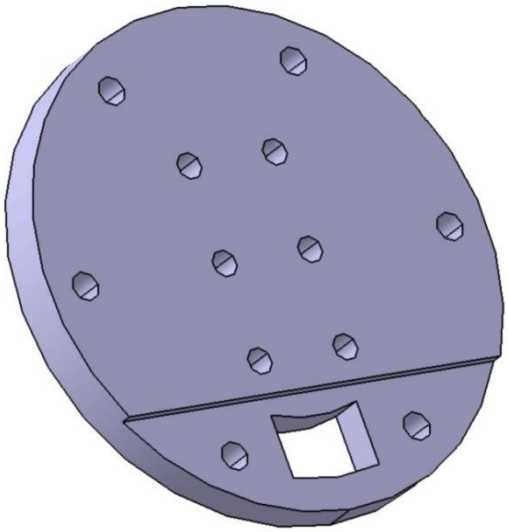

Figure 27 Rear cover

Items 4 and 22 are rubber seals which are used to help to the protection of motor and gearbox from dirt and water. Technical drawing of the parts can be found at the Appendix A.

Item 5 is the motor which is chosen at the previous section. The shaft of the motor is shortened to 9 mm. And items 9 to 13 are the parts of the gearbox.

Item 6, motor holder, which is illustrated in Figure 28, is used to fasten the motor to the inner hub. The detailed drawing of the part can be seen at Appendix A

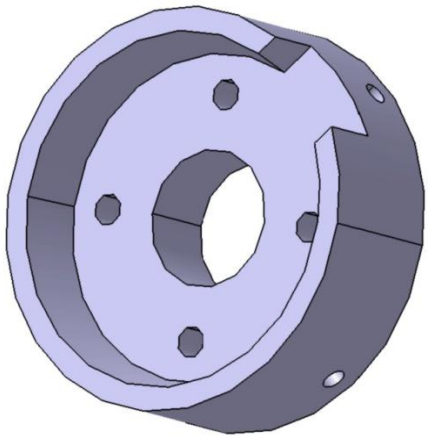

Figure 28 Motor holder

Item 7, coupling, is used to convert the motor shaft diameter to gearbox sun gear input diameter. Technical drawing of the part can be found at the Appendix A.

Item 8, gear box rear holder is used for filling the space between the motor holder and the gearbox itself. Technical drawing of the part can be found at the Appendix A.

Item 15 is the output shaft which transmits the power from gearbox to the outer rim. Technical drawing of the part can be found at the Appendix A.

Item 16 is the output shaft holder, as it helps to hold the shaft in position. Technical drawing of the part can be found at the Appendix A.

Item 18 is the inner case hub, which is illustrated in Figure 29. It houses the motor and the gearbox. The outside environment forces acting on the wheel is transferred to the inner case hub via the bearing, item 19, which supports the outer rim and the output shaft of the gearbox. Technical drawing of the inner case hub can be found at the Appendix A.

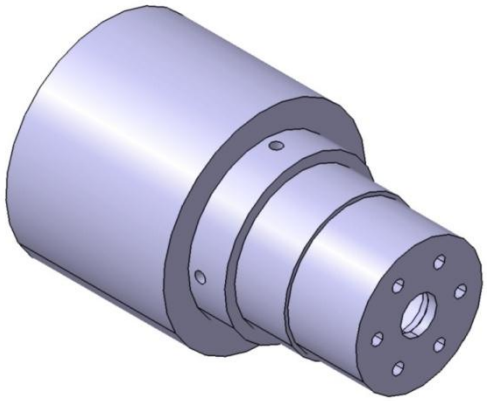

Figure 29 Inner hub case

Item 20 Bearing holder is used to fix the item 19 bearing in its position. This part is fastened to the inner case hub. Technical drawing of the part can be found at the Appendix A.

Tire is fixed by item 21, rim primary part. The rim primary part is supported by the item 19 bearing and item 26 Rim secondary part for the forces transferred from the tire. Technical drawing of the rim primary part can be found at the Appendix A.

The items 23 to 25 are used to connect the rim secondary part with output shaft of gearbox.

Item 26, rim secondary part is used to transfer the power from motor to the rim primary part. Technical drawing of the rim primary part can be found at the Appendix A.

The robot platform body is built by using aluminum sigma profiles as frames and machined parts as anchor points. The rest of the body is covered with aluminum sheet metal as a skin. The exploded view of a module robot platform with the module connection part is illustrated in Figure 30.

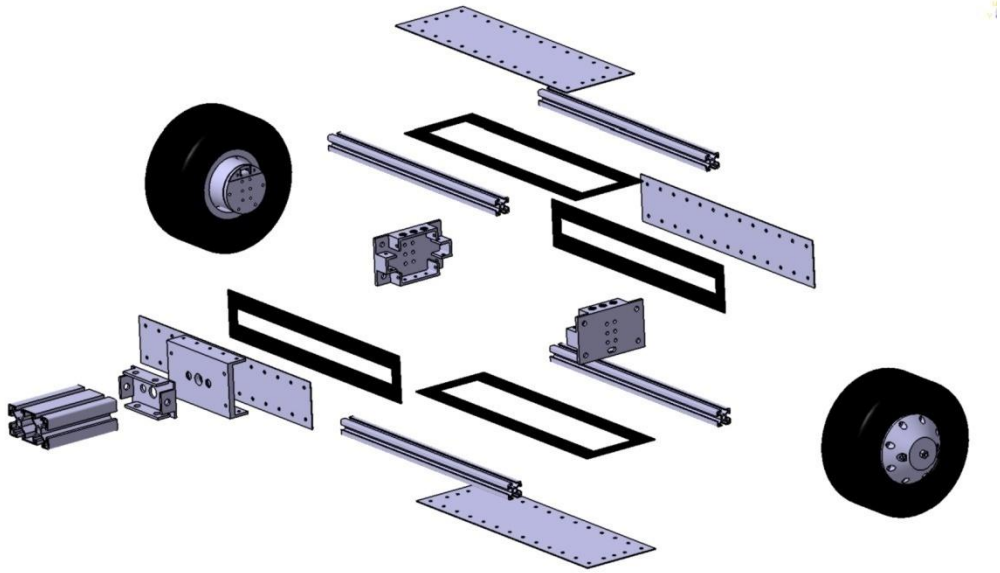

Figure 30 Exploded view of the base robot module with its rigid connection parts

The outside dimensions of a module for this example are designed as 35 cm by 10.4 cm by 6.5 cm. This configuration gives the robot module a ground clearance of 5.5 cm and ability of turning upside down without a problem since the design is axisymmetric. The 20mm by 20mm sigma profiles are used for the frames of the module and 40 mm by 80 mm profiles are used at the module connection. There are

three important machined parts which are designed to hold the whole system together. The detailed drawing of these parts can be seen at Appendix A.

This first one of the machined parts is the module side cover, which is illustrated in Figure 31. It is used to hold together the sigma profiles that form the frame of the module and also the wheels are connected to these parts.

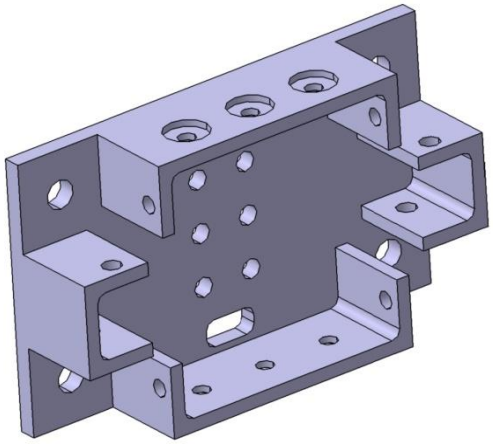

Figure 31 Side cover of the robot module

The second machined part, Figure 32, is the primary connection part. This part is provide connection to the module at one side and provide connection to the rigid module connector, and secondary connection part at the other side.

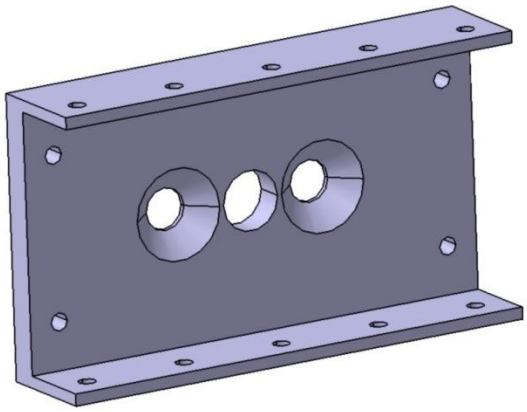

Figure 32 Primary connection part of the robot module

The third connection part is the secondary connection part, which illustrated in Figure 33. The purpose of this part is to provide additional strength to the connector profile and module assembly.

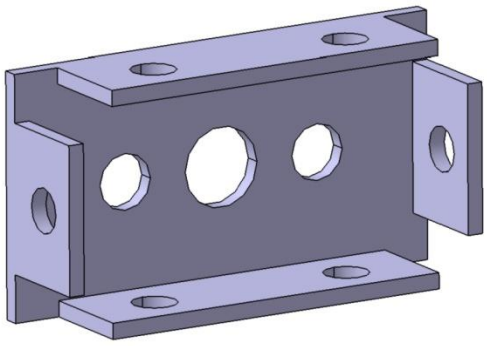

Figure 33 Secondary connection part used at the robot module connection

4.3. Suspension Design

The current designed robot platform is intended for a ruggedized usage which means the components inside body have to withstand sever conditions such as vibration. In order to reduce the effects of the outside environment, it is determined to create a suspension system that can be used at the two wheeled robot module base and can perform its operation even if the robot module turns upside down.

The problem in this goal is that, the current conventional suspension system cannot perform their function when the suspended platform turns upside down because of the fact that the spring is compressed in only one direction of the tire displacements. In other words, the spring part of the spring damper system works only in one direction.

A solution to this problem is found by using a pair of suspension systems in conjugate with each other. The conceptual solution is illustrated in Figure 34. At this solution the outside casing of the suspension works as the base of the platform. The suspension system itself contains a pair of two suspensions, which is illustrated in Figure 35. Each suspension pair is connected from their top and bottom with a connector, which can slide inside the casing and, a pin is attached to each connector which transfers the vertical motion of tire in only in direction and move freely in the other. There are four pins at the suspension. When the tires move up or down with respect to the main body two of the pins force the connectors to move inside thus creates a resistance force and the other two pins moves freely without creating a resistive force. Although this initial design fulfills requirements, it requires relatively large amount of volume and the sliding surfaces must be smooth enough to prevent clogging.

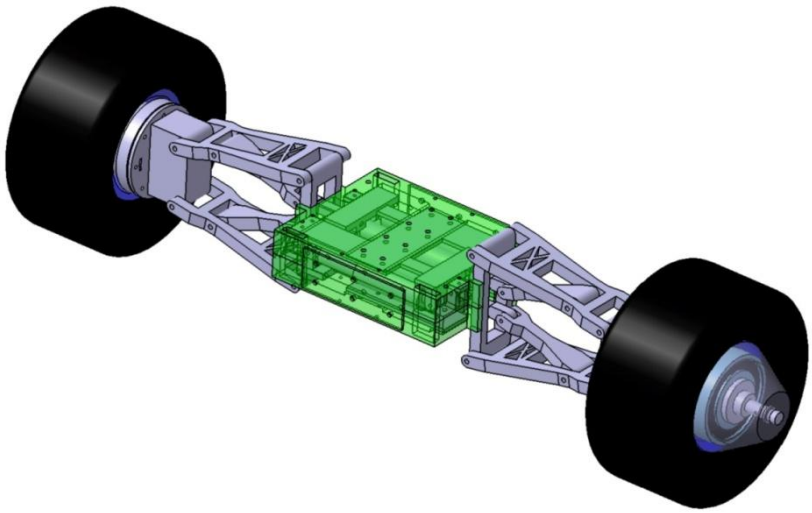

Figure 34 A double sided suspension solution

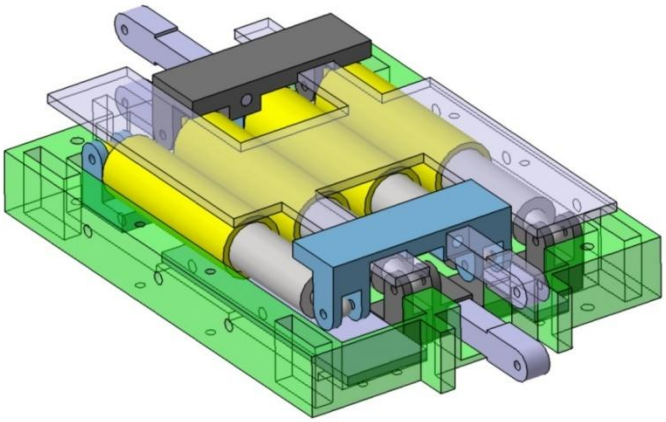

Figure 35 Inside view of the suspension design

Due to the stated problems before, the described suspension design concept is discarded. A new double sided symmetrically working concept is designed which is based on compressing the spring damper system whether the tire moves up or down relative to the main body. A Patent application is filed for the new design.

4.4. Control System Design

In the scope of this thesis a simple controller system is implemented to the robot platform in order to perform low level actions like move forward, backward of turn.

The control system mainly consists of a PIC microcontroller card, two commercial brushless motor electronic speed controllers on each module, and one wireless RS232 protocol transmitter for each module. The schematic of the microcontroller card is given in Figure 36. PIC 18F4680 class microcontroller is used at this card. The controller card has two Hall Effect sensor connections, which are used as a motor encoder, inputs. It can communicate with the other module's controller cards via the wireless transceiver. The controller card is designed for two battery inputs which are connected to the speed controllers over the card. Voltage and current sensors are placed to these connections in order to monitor the power usage of the motors. The information exchange with the computer is accomplished through RS232 protocol. Also the controller cards can communicate with computer or with each other via RS232 protocol.

The wireless transceiver used at the thesis is Xbee pro module produced by Digi. The Xbee pro module works at 3.3V for this reason a voltage converter is needed while using the PIC micro controller. The module itself has a 1.6 kilometers line of sight and 100 meters indoor range according to its specifications. Although not used at thesis but apart from being a wireless RS232 transceiver, the module has other features like ADC input and digital I/O pins and encrypted communication between modules according to the product specifications [20].

When the robot platform is turned on, controller cards wait an initialization command from the computer. After receiving the initialization command controllers send a confirmation message and then computer sends the command for the actuation of the motors. The actuation command for motors contains one byte, which is actually telling the robot the next codes are related to motor speed and travel distance, and twelve words, which are one word for speed and one word for travel distance per

wheel and three bytes in front of every four word which declares the next four word belongs to a specific module designated by the declaration byte. Every controller card receives this speed and travel duration of each wheel and processes only the commands regarding their own module. Upon the end of computer and module communication each module controller starts to produce servo controller signal for the brushless speed controllers for a period of determined distance which is measured by a Hall Effect sensor placed near to the motor inside the hub. Also every controller card can communicate with each other send commands like emergency stop or a synchronization command, a representation of the controller schematic is given in Figure 37. The computer can also send query commands for information like volt and ampere usage from each module.

Actions done so far can be summarized as the realization steps of the robot platform. In this chapter required motor, battery and gearbox for this platform is selected, and then detailed design of the hub motor concept is shown, after that the body of the robot is described and finally the schematics of the control system explained. Apart from these a conceptual double sided suspension system is shown. The robot platform is manufactured with respect to the defined specification at this chapter and test results of this platform on the real world applications are discussed at the next chapter.

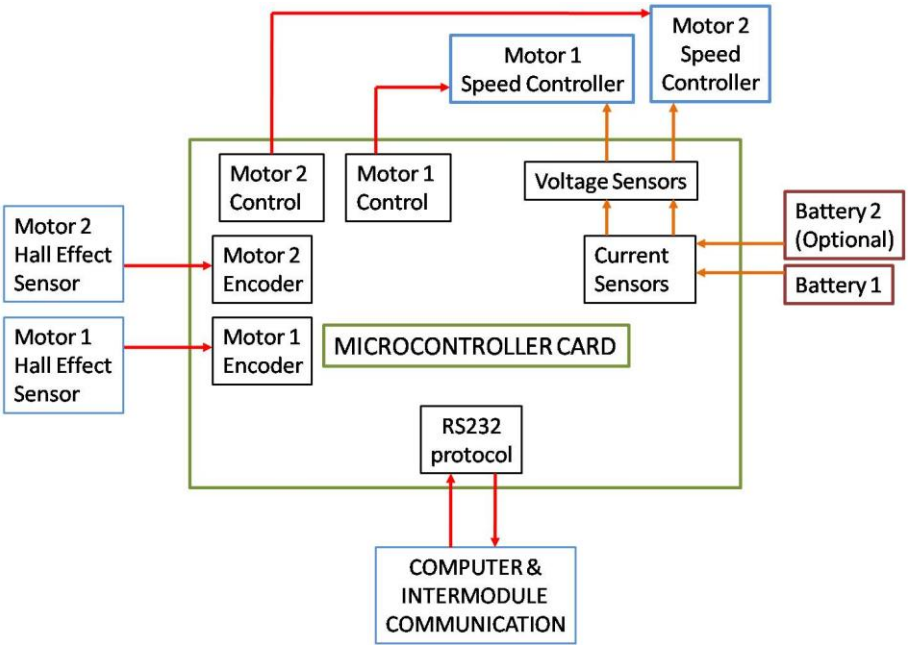

Figure 36 Micro controller card schematic

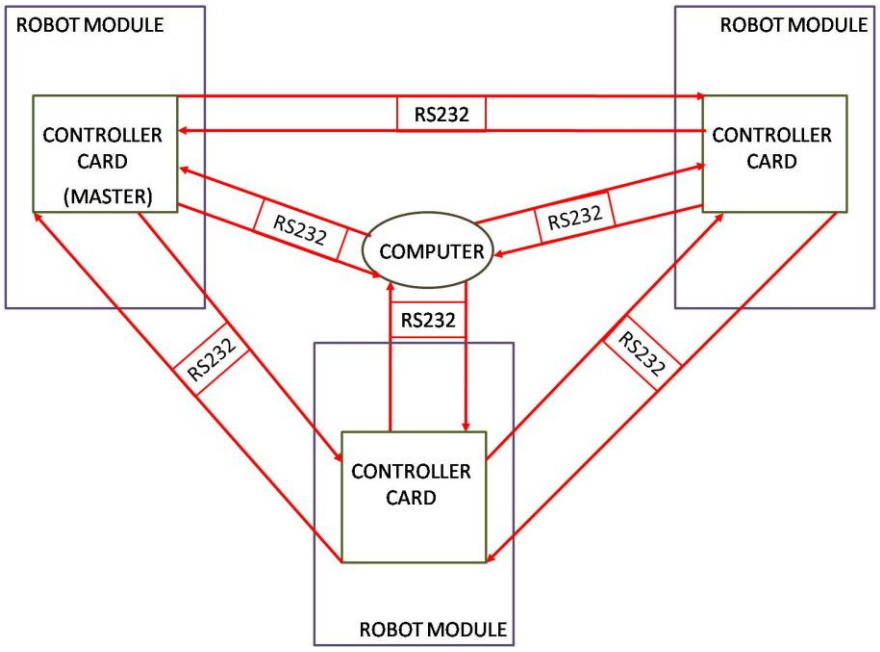

Figure 37 Representation of the robot platform communication schematic

CHAPTER 5

TEST ENVIRONMENT AND RESULTS

In this chapter the test of the manufactured robot platform in real world applications are discussed. The initial functionality tests of the platforms are performed with bodies made of wood, the two wheeled demo module and six wheeled demo module is shown in Figure 38 and Figure 39. These modules are controlled with a standard RC controller. The tests conducted with the prototype platform include climbing a slope, going at an inclined surface and going over a step and gap crossing. The test setup surfaces are coated with sand paper in order to increase the friction constant between the tires and the surface.

Figure 38 Demo two wheeled robot module with its RC controller

Figure 39 Demo three module robot platform with its RC controller

Apart from the experiments used to determine the capabilities of the robot platform, also the stall torque of the motor. As can be seen from Figure 40, the torque measurement setup consist of spring scales tied to the ground at one end and tied to a rope which is wrapped around the wheel at the other end. For the test motor inside the wheel is put into a condition where it can no longer pull the force and then the tension at the rope is read by using spring scales. According the results the motor stall at a situation where 35kgf is applied to a 5cm moment arm. From here the stall torque for one wheel is calculated as 17.2Nm.

The first experiment for the measurement of the physical capabilities of the robot platform is climbing a slope. It is used to find the maximum slope angle that the robot platform can climb, schematic is shown in Figure 41. Setup is constructed by leaning a flat surface to the wall and controlling the distance of its end at the horizontal surface to the wall, which can be seen at Figure 42. The tests showed that the maximum climbable slope degree with this setup is 50˚. At this point the robot platform started to slip.

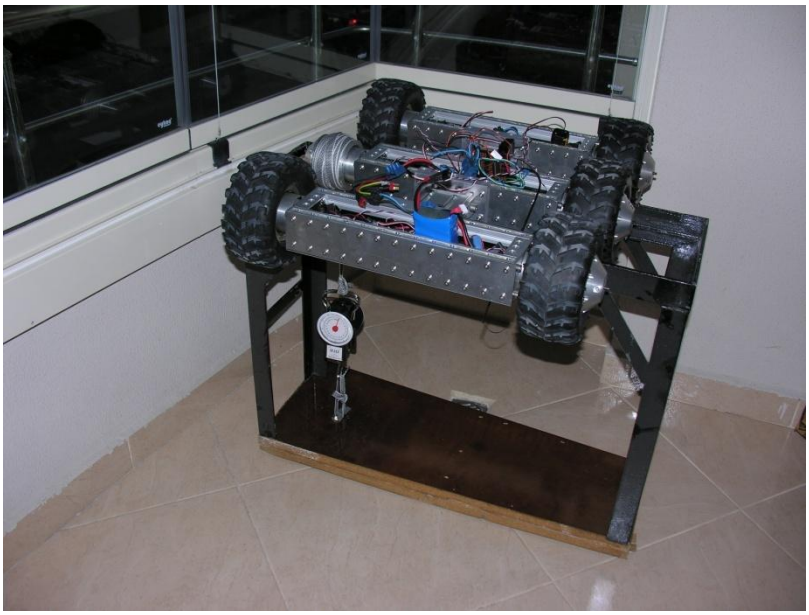

Figure 40 Stall torque measurement experiment setup

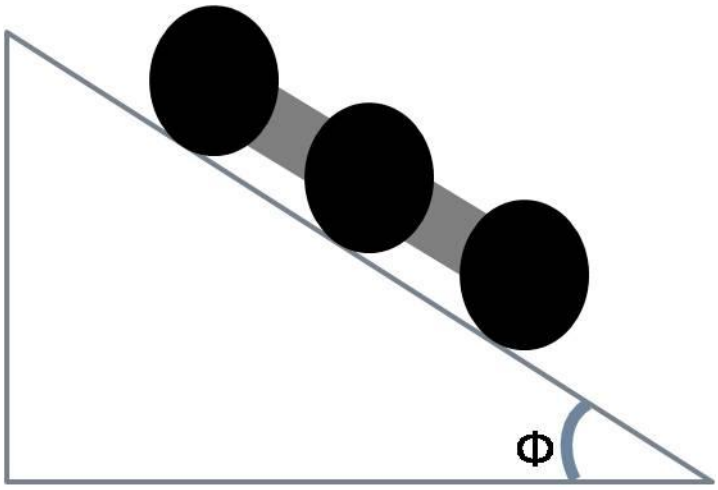

Figure 41 Robot climbing a slope experiment schematic

Figure 42 Robot climbing a slope experiment setup

The second experiment, going at an inclined surface, used for determining the maximum inclined angle that the platform can traverse, schematic of the experiment is given in Figure 43. Setup is constructed by leaning a flat surface to the wall and controlling the distance of its end at the horizontal surface to the wall similar to the first experiment setup, which is shown in Figure 44. The tests showed that the limit of the transversal surface degree with this setup is again 50˚.At this point the robot platform started to slip.

The limiting factor in these both tests is determined as the friction coefficient between the wheel and the surface. The tangent of the maximum climbable slope cannot pass the coefficient of friction value. As long as the vehicle motors provide enough torque to create an equal force to the maximum friction force the vehicle can climb the slope up to the tripping point.

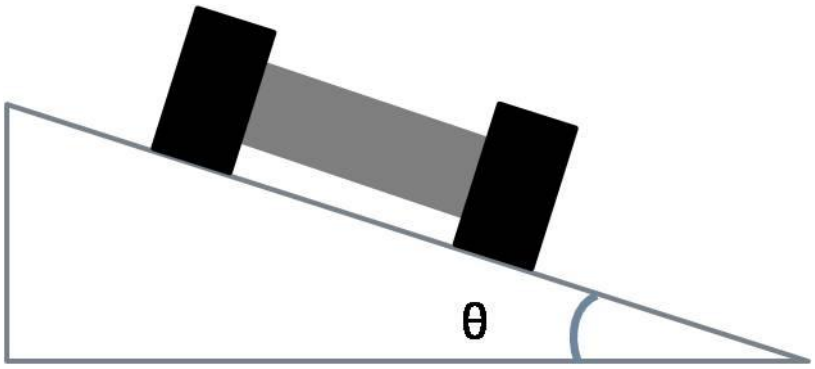

Figure 43 Robot platform going at an inclined surface experiment schematic

Figure 44 Robot platform going at an inclined surface experiment setup

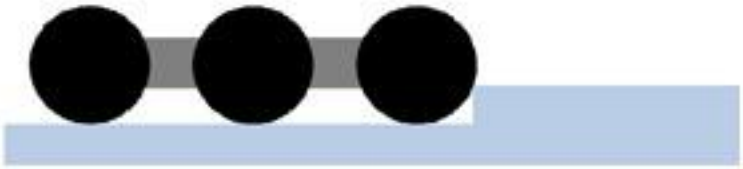

Figure 45 Robot platform going over a step experiment schematic

Figure 46 Robot platform going over a step experiment setup

The third conducted test is the obstacle climb test. It is aimed to measure the maximum height of an obstacle which the robot platform can climb, schematic of the

test is given in Figure 45. The test setup, which is shown in Figure 46., consists of a vertical obstacle surface and an upper platform. For the test vertical obstacle surfaces are prepared in various heights. The upper platform height can be adjusted to match the height of the vertical obstacle surface. The theoretical maximum height can be calculated using the static equilibrium equations for the acting forces on the robot platform which are shown at the Figure 47. At verge of going over maximum step height it is assumed that no force is acting on the rear wheel from lateral surface and wheels provide enough torque to get maximum friction force from the surfaces and also the system is at static equilibrium. From here the related force equations are as follows:

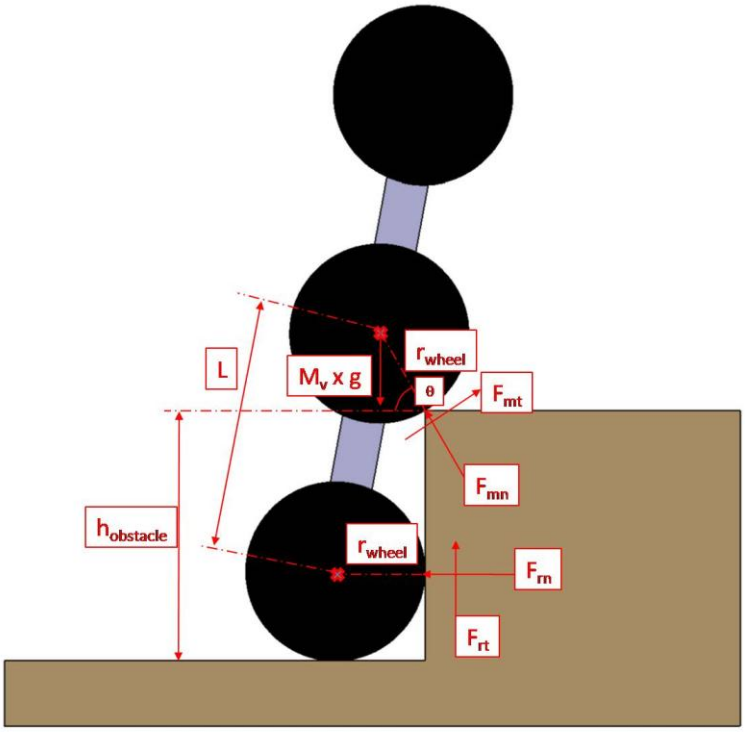

Figure 47 Forces acting on the robot platform going over a step

$$\sum F_x = 0 = -F_{rn} + F_{mt} \times \sin\theta - F_{mn} \times \cos\theta \quad (5.1)$$

$$\sum F_y = 0 = F_{rt} + F_{mt} \times \cos\theta - F_{mn} \times \sin\theta - M_v \times g \quad (5.2)$$

$$\sum M = 0 = -M_v \times g \times r_{wheel} \times \cos\theta - F_{rn} \times (h_{obstacle} - r_{wheel}) \quad (5.3)$$

$$F_{rt} = F_{rn} \times \mu \quad (5.4)$$

$$F_{mt} = F_{mn} \times \mu \quad (5.5)$$

$$\theta = \tan^{-1}\left(\frac{r_{wheel}}{h_{obstacle} - r_{wheel}}\right) + \cos^{-1}\left(\frac{2 \times r_{wheel}^2 + (h_{obstacle}^2 - r_{wheel}^2) - L^2}{2 \times r_{wheel} \times \sqrt{(h_{obstacle} - r_{wheel})^2 + r_{wheel}^2}}\right) - 90 \quad (5.6)$$

Where:

F_{mn} : Normal force on the middle wheel

F_{mt} : Maximum friction force on the middle wheel

F_{rn} : Normal force on the rear wheel

F_{rt} : Maximum friction force on the rear wheel

$h_{obstacle}$: Height of the obstacle

L : Length between the centers of the wheels

M_v : Total mass of the robot platform

μ : Coefficient of friction between tire and the surface

θ : Angle of the normal force on the middle wheel with lateral surface

For a 17.2kg total robot platform weight, a 1.19 coefficient of friction, a 8.5cm wheel radius and a 23cm length between the wheel centers the maximum theoretical climbable step height is calculated as 23.6cm. But in the tests it is seen that maximum climbed step height of the robot platform is around 20-23cm, that is the robot platform could climb 20cm but couldn't climb the 23 cm step height at the tests. The discrepancy between the theoretical and the real world test results can be

the result of the probable difference between the real world and theoretical values of the friction force on the middle wheel or due to the wheels that act like a spring during impact to the obstacle.

The last performed test in the scope of the thesis is the gap crossing test. It is aimed to determine the maximum gap width that the robot platform can pass without falling into the gap, schematic of the test is given in Figure 48. As can be seen from the Figure 49 the test setup consists of two flat surfaces where the difference between them can be altered. The tests showed that robot platform can cross 35cm gap but it fails at crossing a 39cm gap.

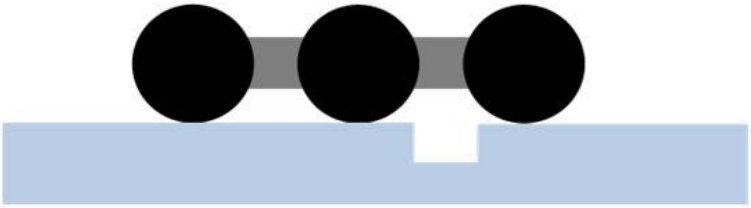

Figure 48 Robot platform gap crossing experiment schematic

Figure 49 Robot platform gap crossing experiment setup

Table 4 Conducted test results

Tests	Maximum achieved Value
climbing a slope	50 degree
transversal of an inclined surface	50 degree
going over step	between 20 and 23cm
gap crossing	between 35 and 39cm

To sum up in this chapter physical capabilities of the platform are tested. Mainly four tests are conducted, which are climbing a slope, going at an inclined surface, going over a step and gap crossing. The tests showed that the robot platform design satisfy the minimum design requirements. The results of the tests can be seen at Table 4. Conclusion is given and future work is discussed at the next chapter.

CHAPTER 6

CONCLUSION AND FUTURE WORK

In this thesis it is aimed to create a low cost, all terrain modular robot platform, using commercial components, in order to fill the need of an affordable robot platform with a wide application area. The initial survey revealed that the best traverse capability versus load carrying capacity is obtained at man portable sized robotic platforms. For this reason the size factor of the designed robot is determined as a man portable platform.

Several example robot platforms, with different locomotion systems, are found and inspected at the further literature search in this robot size factor. The specifications of the robot platform are determined based on the properties of the robots inspected at the literature survey. From here it is defined that the robot platform is formed from two wheeled modules and each module has a maximum 2.8kg payload carrying capacity; it has a maximum speed between 0.6 and 1.2 m/s and can climb 45° slope. Based on these specifications several platform concepts are described with smaller than hub module bodies which enable the ability to move even if module is turned upside down and varying degrees of freedom at the joints of the modules and different locomotion systems. A three module wheeled robot platform with rigid connections between the modules is selected as a test platform due to its relative simplicity with respect to the other configurations.

The detailed design of the selected test robot platform is done. For the motor, speed controller and wheel, RC plane and car parts are used due to their low cost, short procurement times, standard size and connection of the products and ever increasing aftermarket product alternatives. The aftermarket gearbox of the Einhell brand electric hand screw is selected for gearbox of the robot platform with similar reasons of the wheel, motor and controller selection. Also a simple electronic

system is designed for the robot controls which takes the commands from the computer via RS232 over wireless connection and moves the robot forward, backward, or rotates the robot platform. A sample platform is manufactured based on the completed designs and its performance is tested at real application platforms.

In the future work the rigid connectors between the modules is planned to be replaced with one or two degree of freedom connectors. The wireless RS232 communication with the computer will be replaced with a more reliable system. A more advanced controller card will be designed to handle various sensors that will be placed inside robot platform and interface with the embedded computer that will be placed inside the platform in order to form a more autonomous platform.

REFERENCES

[1] Carnegie Melon University National Robotics Engineering Center web site, http://www.rec.ri.cmu.edu/projects/crusher/Crusher_Brochure.pdf, Last access date 12 January 2010.

[2] Aselsan İzci Unmanned Ground Vehicle web site, http://www.aselsan.com.tr/urun.asp?urun_id=236&lang=en, Last access date 12 January 2010.

[3] Foster-Miller Company Talon robot product brochure, http://www.foster-miller.com/literature/documents/TALON-Brochure.pdf#talon_brochure, Last access date 12 January 2010.

[4] Wikipedia Talon robot introduction web site, http://en.wikipedia.org/wiki/Foster-Miller_TALON, Last access date 12 January 2010.

[5] Chaos robot image website, http://autonomoussolutions.com/Images/products/Chaos/MoreImages/Chaos5.jpg, Last access date 12 January 2010.

[6] Autonomous Solutions company Chaos robot product web site, http://www.autonomoussolutions.com/products/chaos.php, Last access date 12 January 2010.

[7] Mesa Robotics Company Matilda performance specifications sheet, http://www.mesa-robotics.com/files/MATILDA%20Performance%20Spec.pdf, Last access date 12 January 2010.

[8] iRobot company Packbot mapping kit specifications sheet, http://www.irobot.com/filelibrary/pdfs/gi/robots/iRobot_PackBot_Mapping.pdf, Last access date 12 January 2010.

[9] iRobot company Packbot product information web page, http://www.irobot.com/sp.cfm?pageid=171, Last access date 12 January 2010.

[10] Mobile Robots Company website, http://www.activrobots.com/ROBOTS/systems.html, Last access date 12 January 2010.

[11] Mobile Robots Company product specifications comparison web page, http://www.activrobots.com/ROBOTS/specs.html, Last access date 12 January 2010.

[12] K-TEAM corporation Koala II robot specifications web page, http://www.k-team.com/kteam/index.php?site=1&rub=3&upPage=94&page=18&version=EN, Last access date 12 January 2010.

[13] AAI Canada Inc. Gaia-2 robot platform product web page, http://www.aai.ca/robots/gaia_2.html, Last access date 12 January 2010.

[14] The Machine Lab Inc. MMP-8 robot platform product web page, http://www.themachinelab.com/MMP-8.html, Last access date 12 January 2010.

[15] The Machine Lab Inc. product comparison web page, http://www.themachinelab.com/MMPComparison.html, Last access date January 2010.

[16] Bayar, Gökhan “Configurable Robot Base Design For Mixed Terrain Applications”, Ms. C., Middle East Technical University, 2005.

[17] Galileo robot press web page, http://www.galileomobility.com/wp-content/uploads/2009/01/ViperRobotMagArticle.pdf, Last access date 12 January 2010.

[18] Galileo robot picture web page, http://www.galileomobility.com/wp-content/uploads/2008/08/viperproducs.jpg, Last access date 12 January 2010.

[19] Genta, G., Motor Vehicle Dynamics, World Scientific, 1997.

[20] Xbee Pro web page, http://www.digi.com/pdf/ds_xbeemultipointmodules.pdf, Last access date 28 April 2010.

APPENDIX A

TECHNICAL DRAWING OF THE PARTS

Technical drawings of the wheel parts and module connector parts are given in the Appendix at figures from 50 to 66.

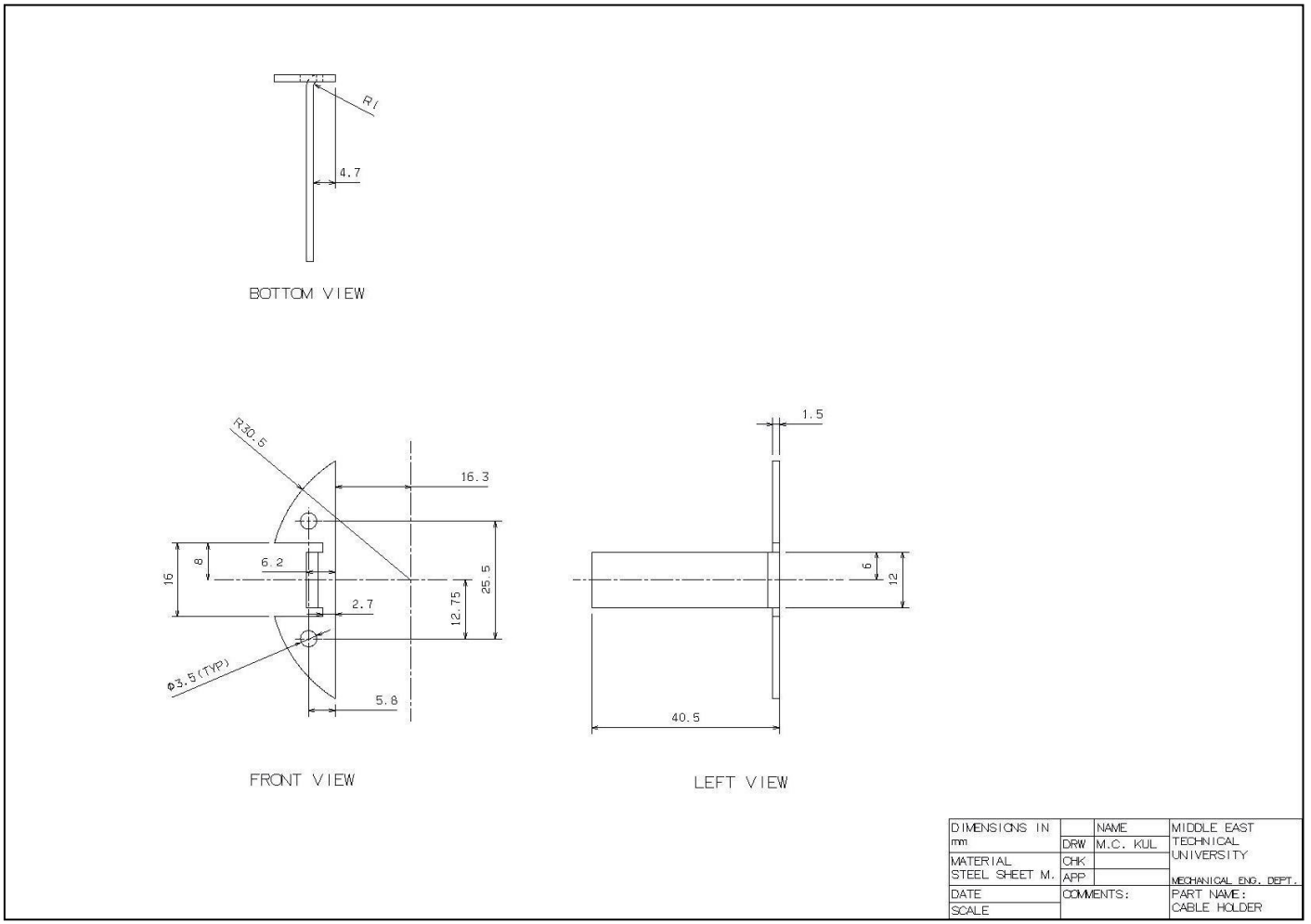

Figure 50 Cable holder technical drawing

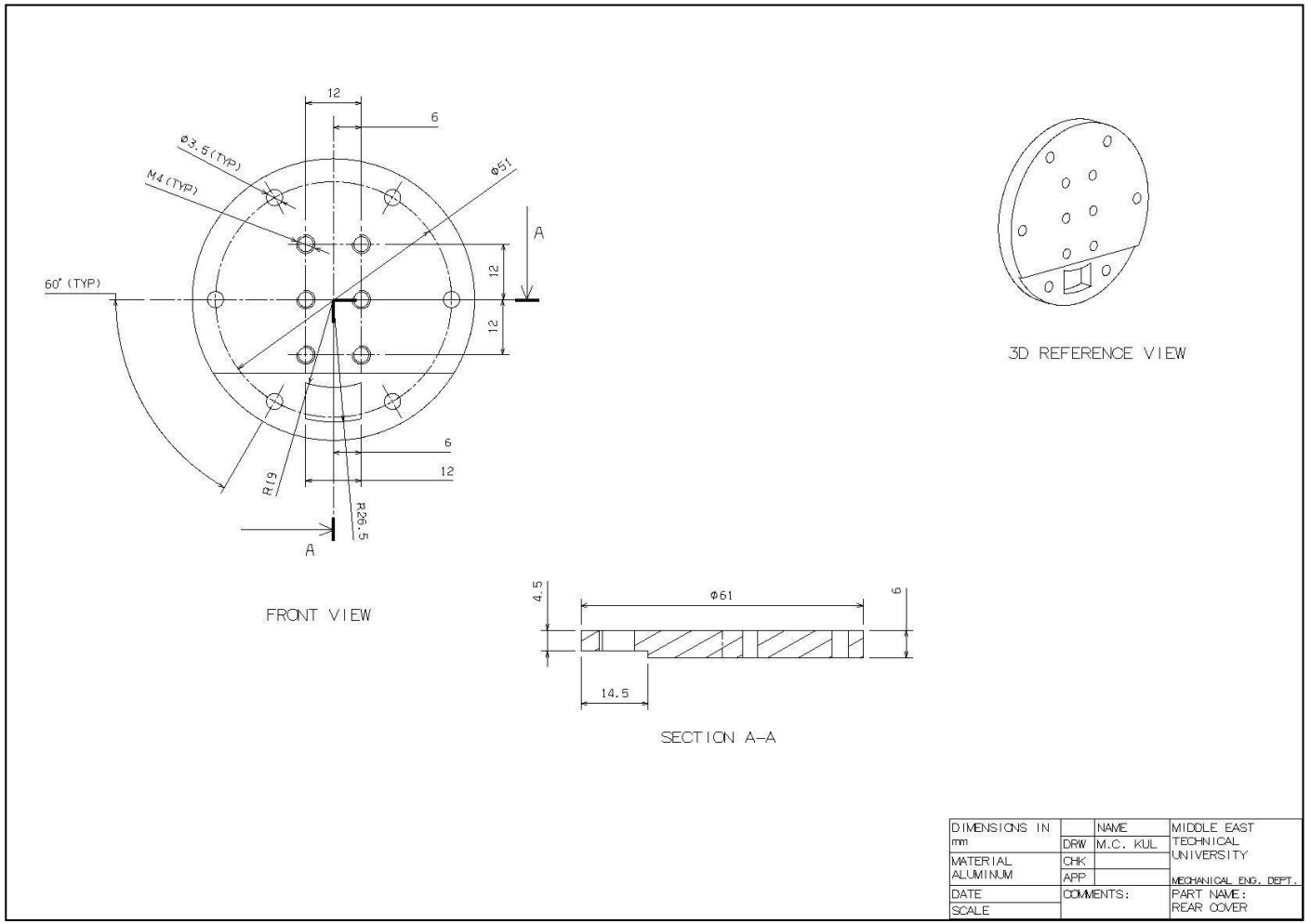

Figure 51 Rear cover technical drawing

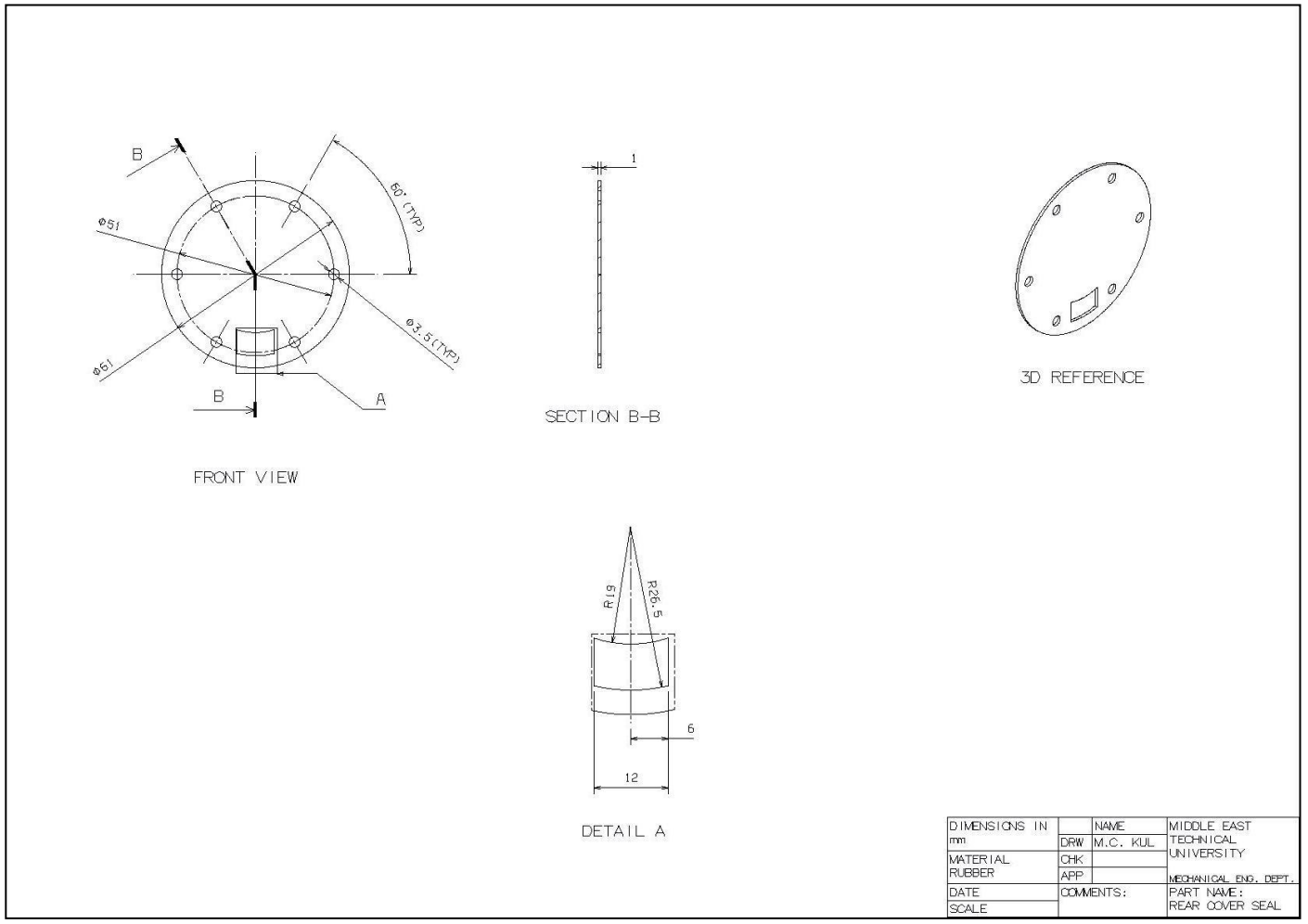

Figure 52 Rear cover seal technical drawing

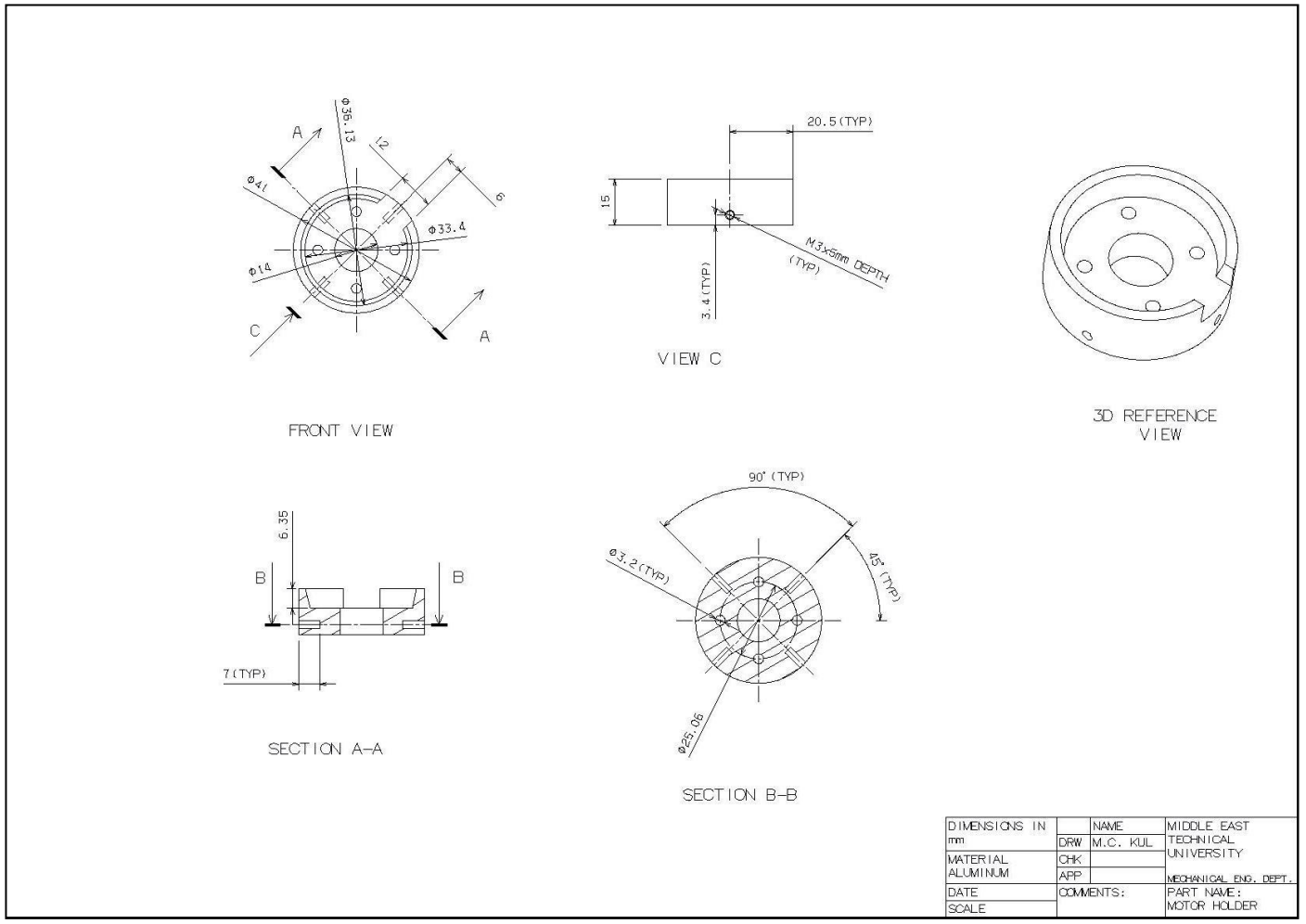

Figure 53 Motor holder technical drawing

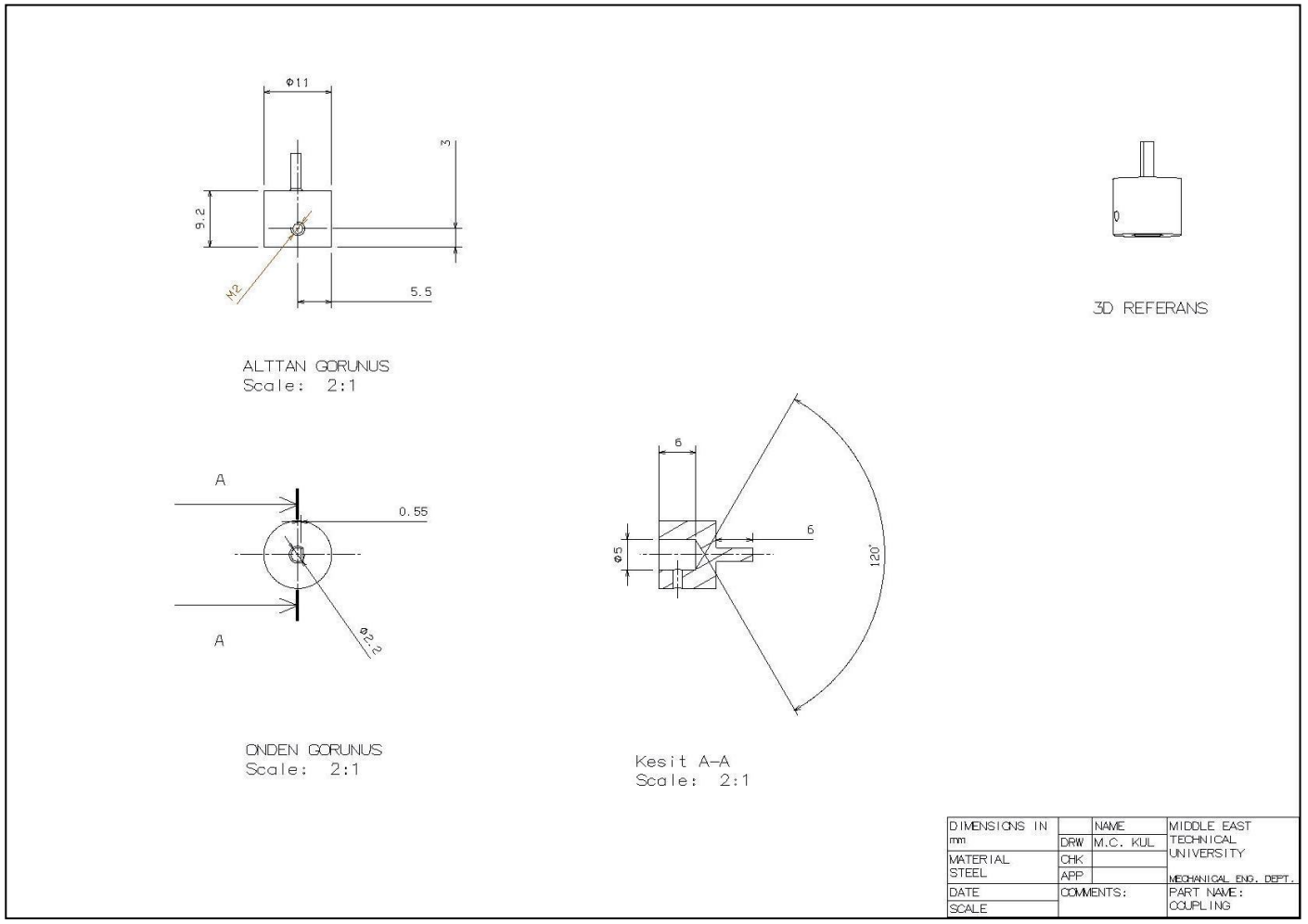

Figure 54 Coupling technical drawing

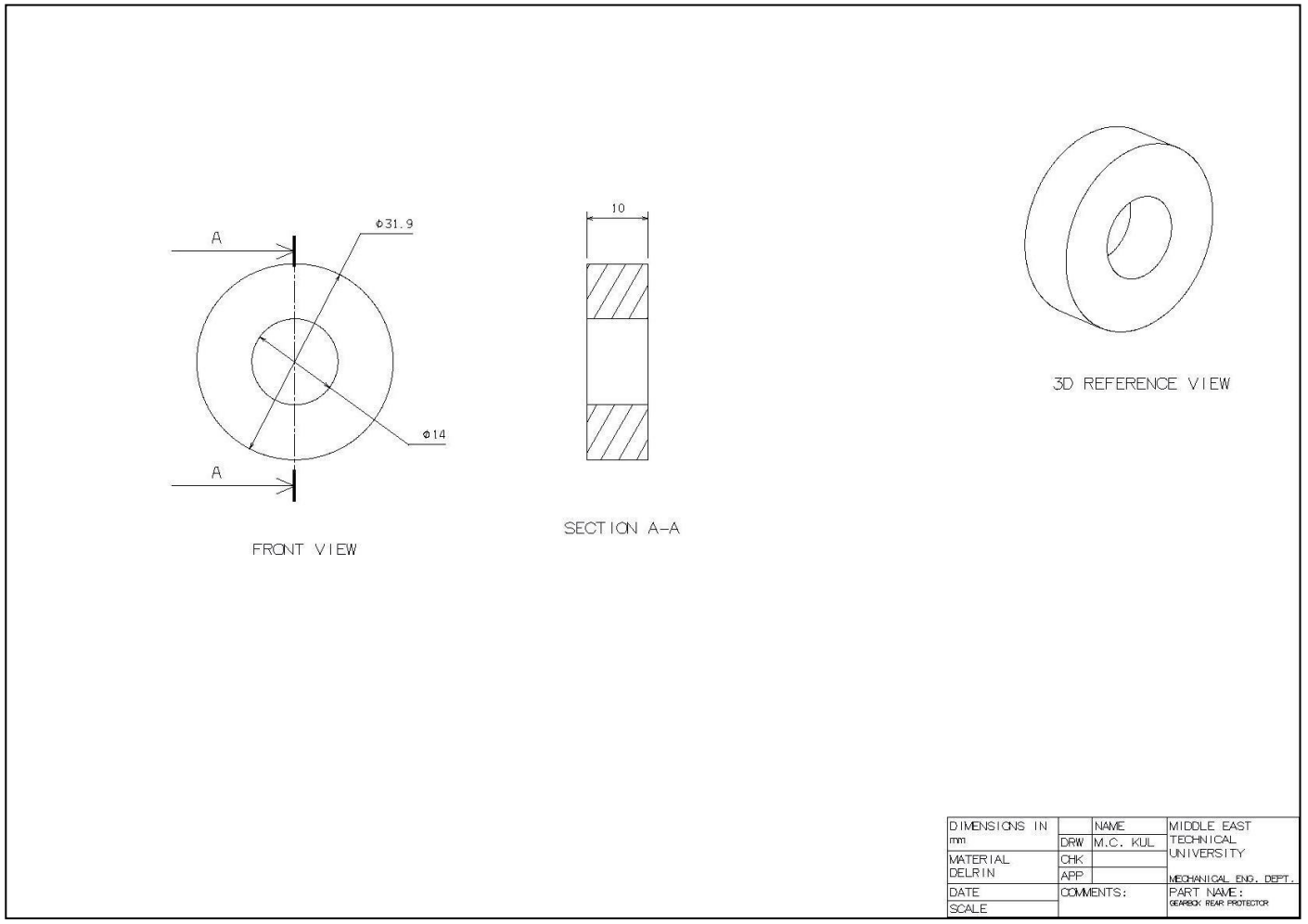

Figure 55 Gearbox rear protector technical drawing

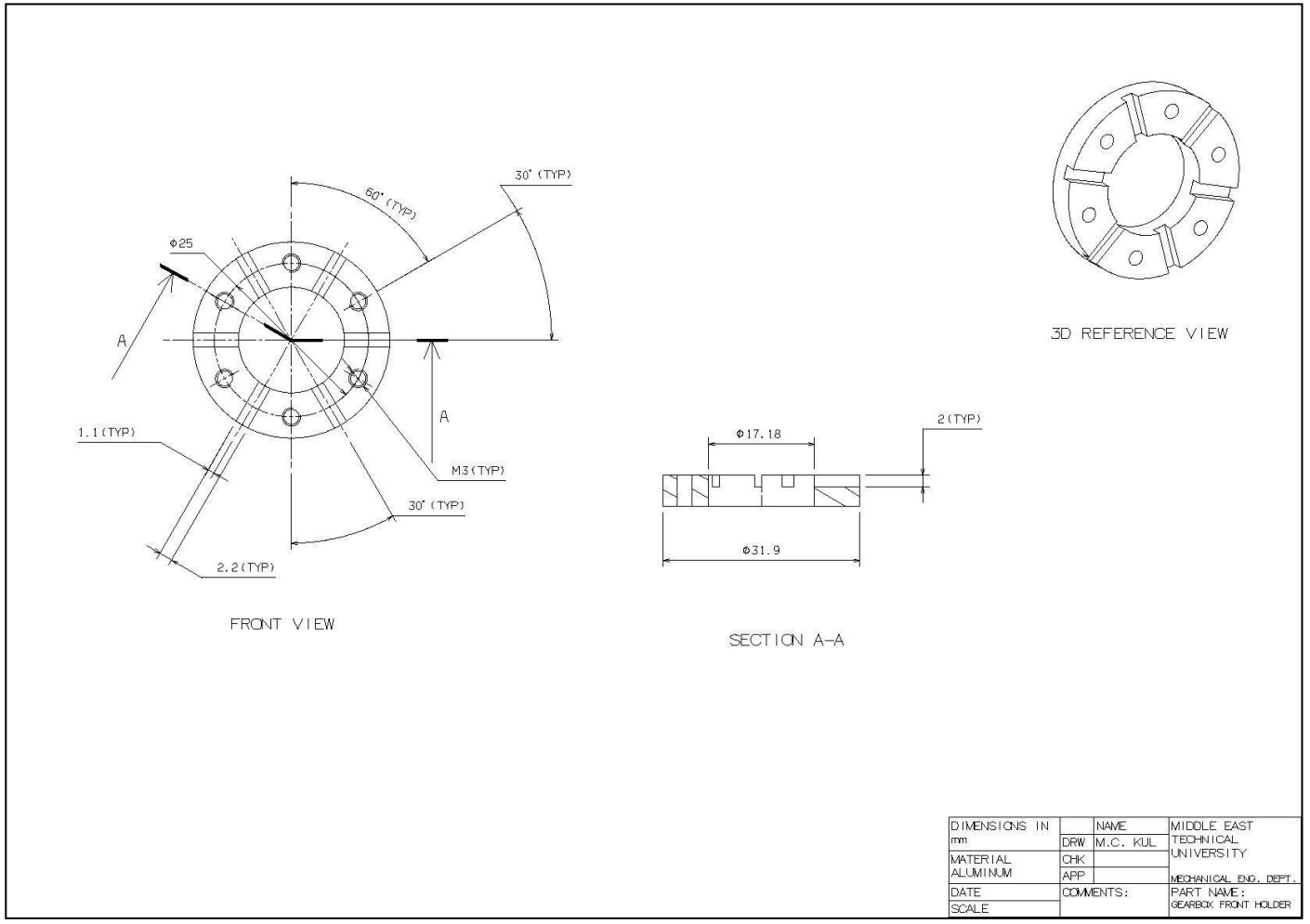

Figure 56 Gearbox front holder technical drawing

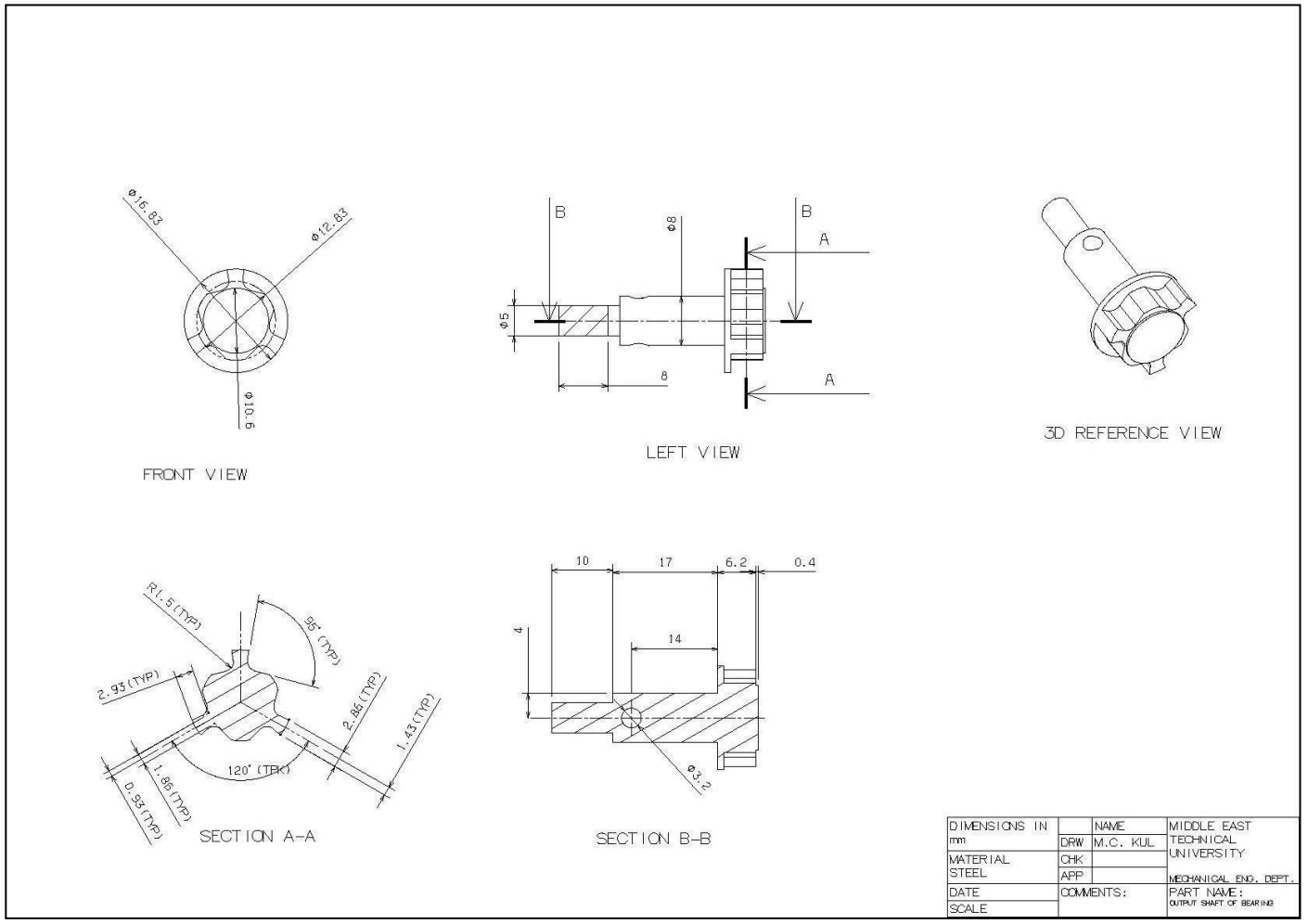

Figure 57 Output shaft bearing technical drawing

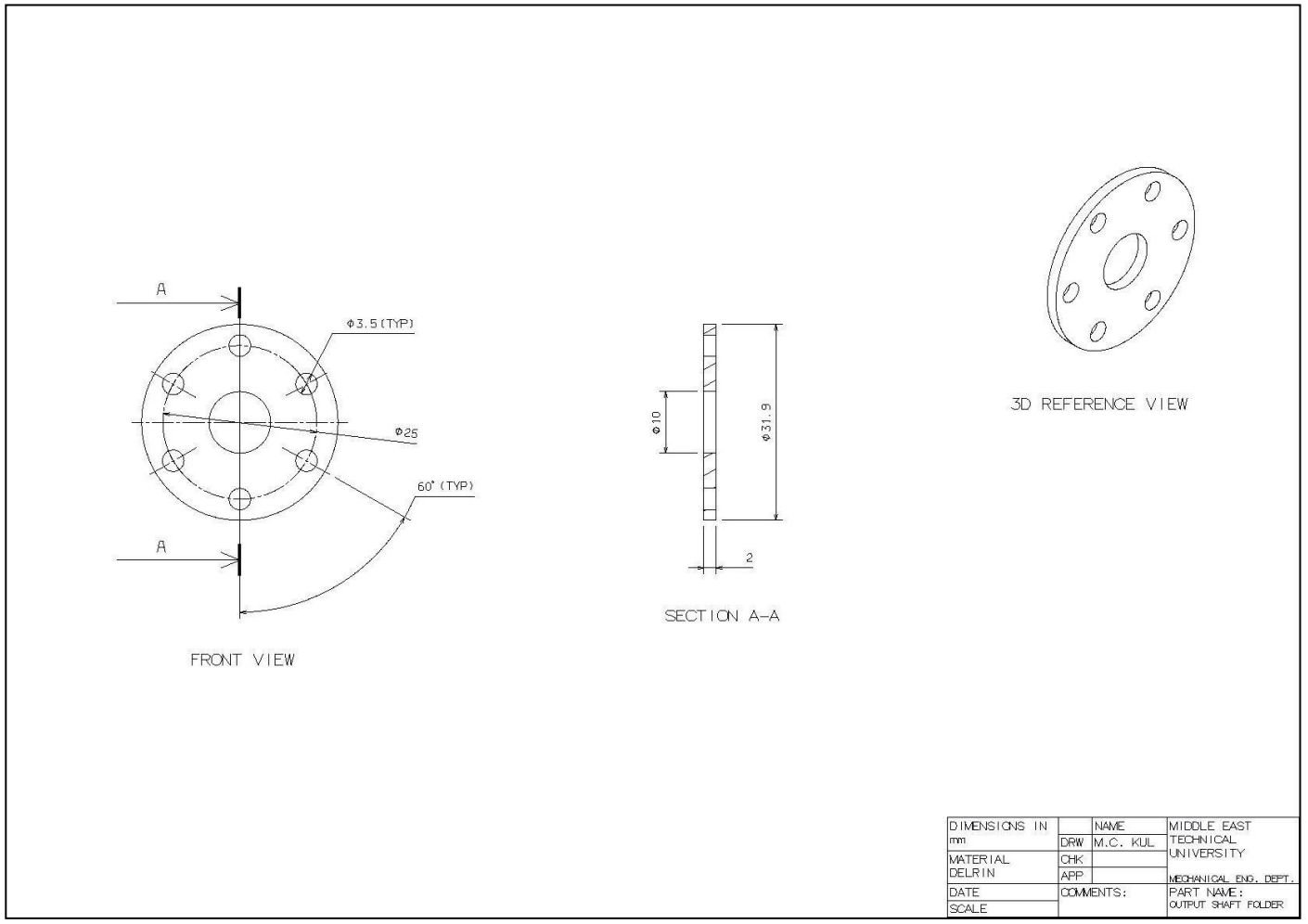

Figure 58 Output shaft holder technical drawing

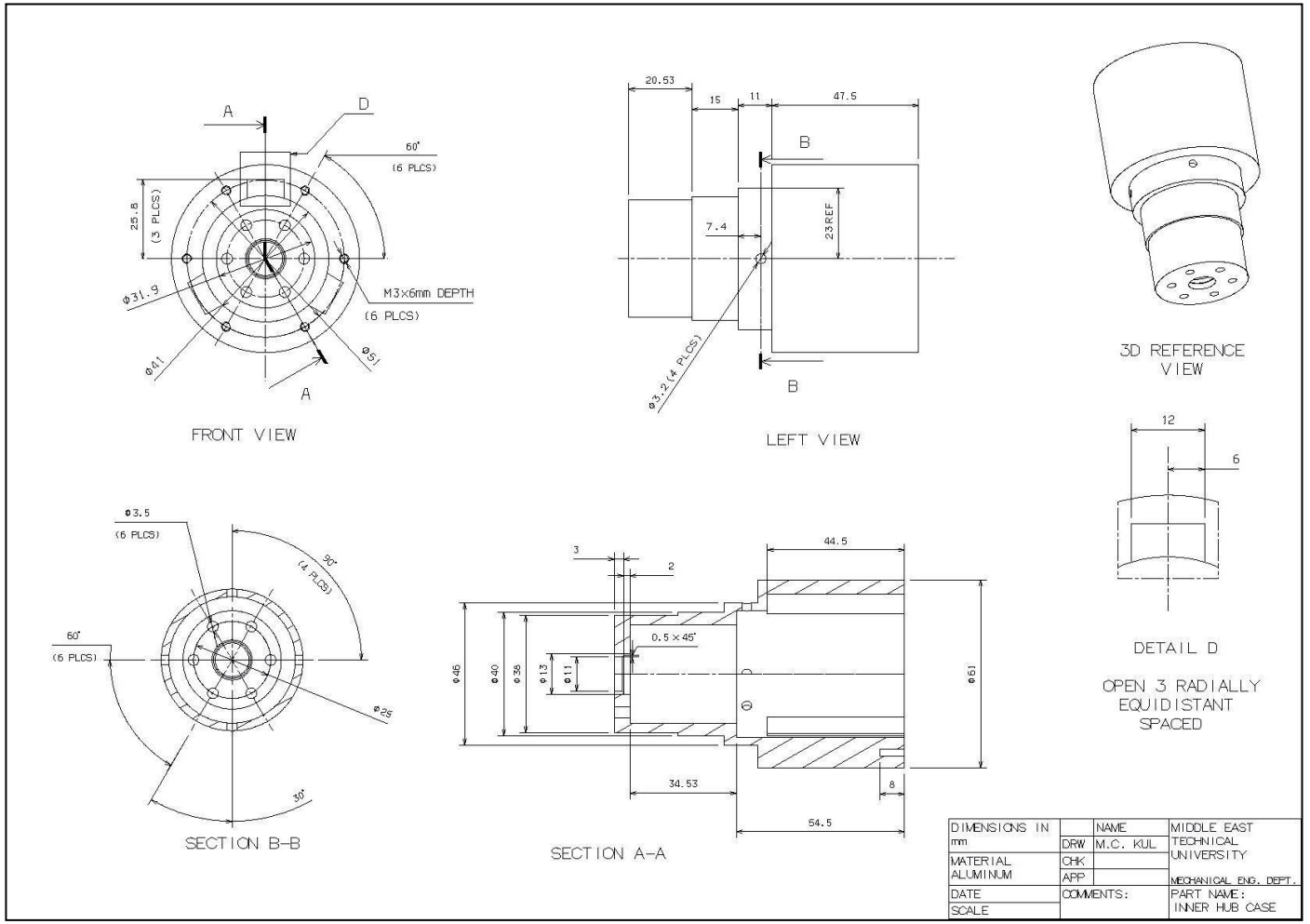

Figure 59 Inner hub case technical drawing

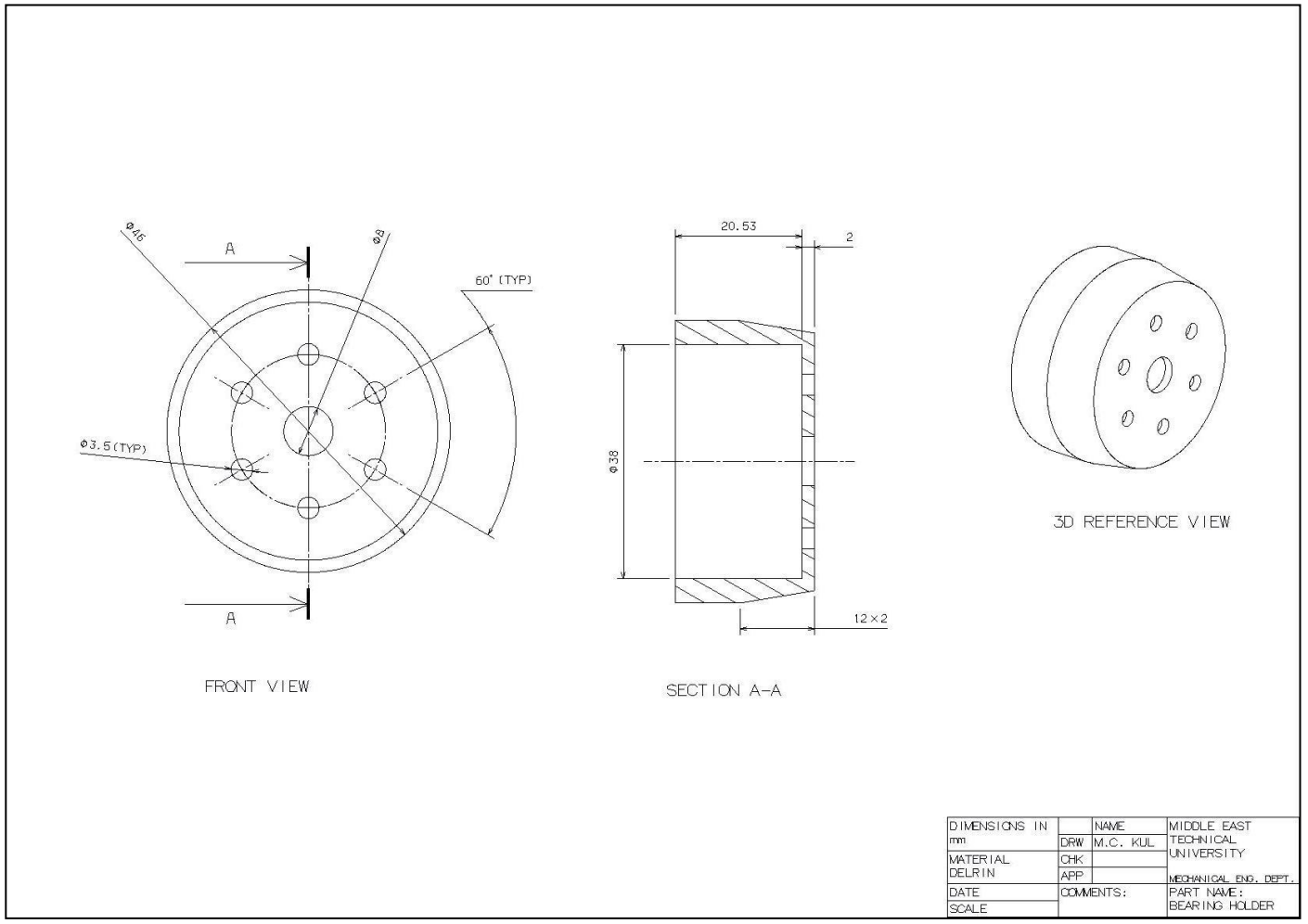

Figure 60 Bearing holder technical drawing

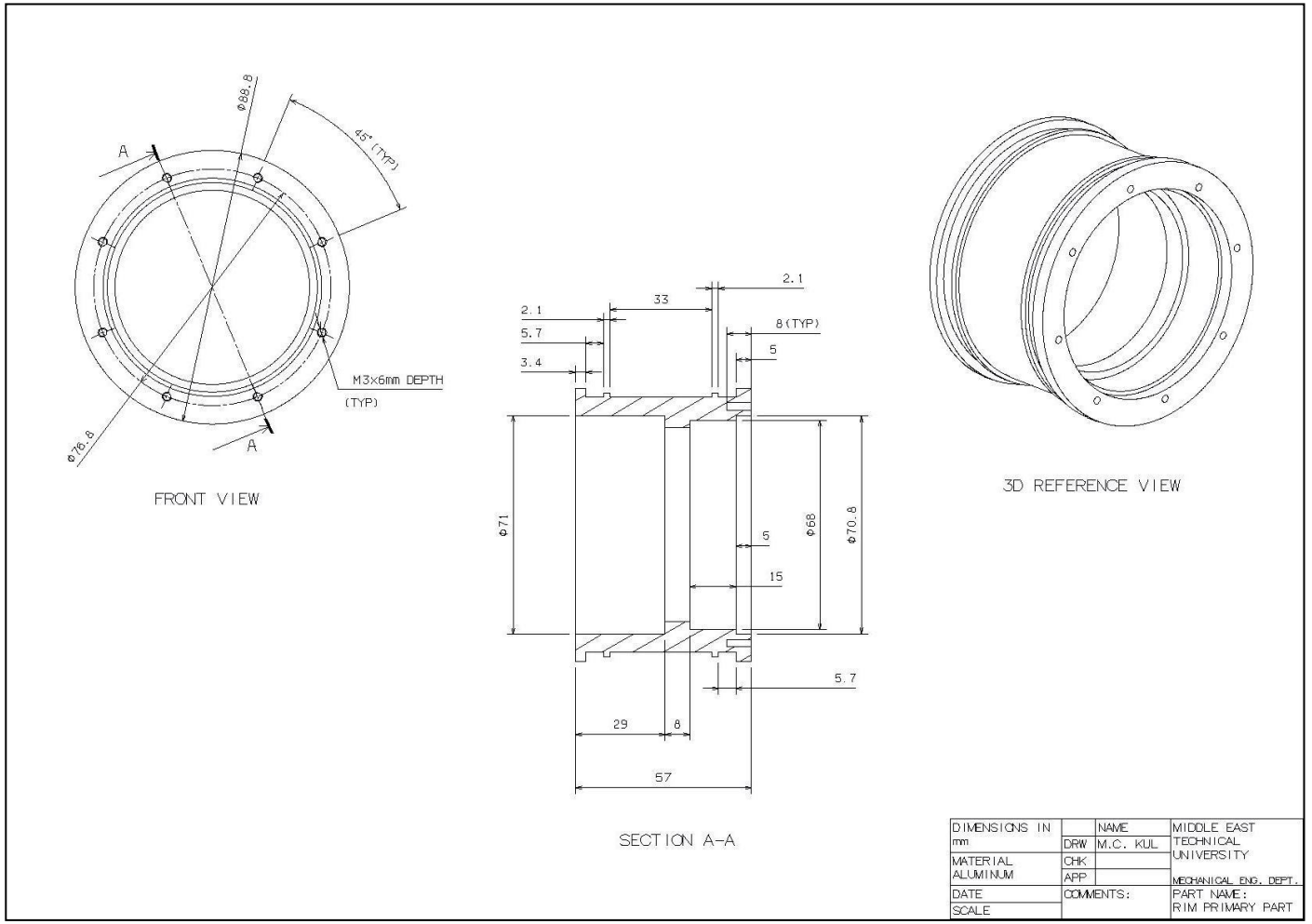

Figure 61 Rim primary part technical drawing

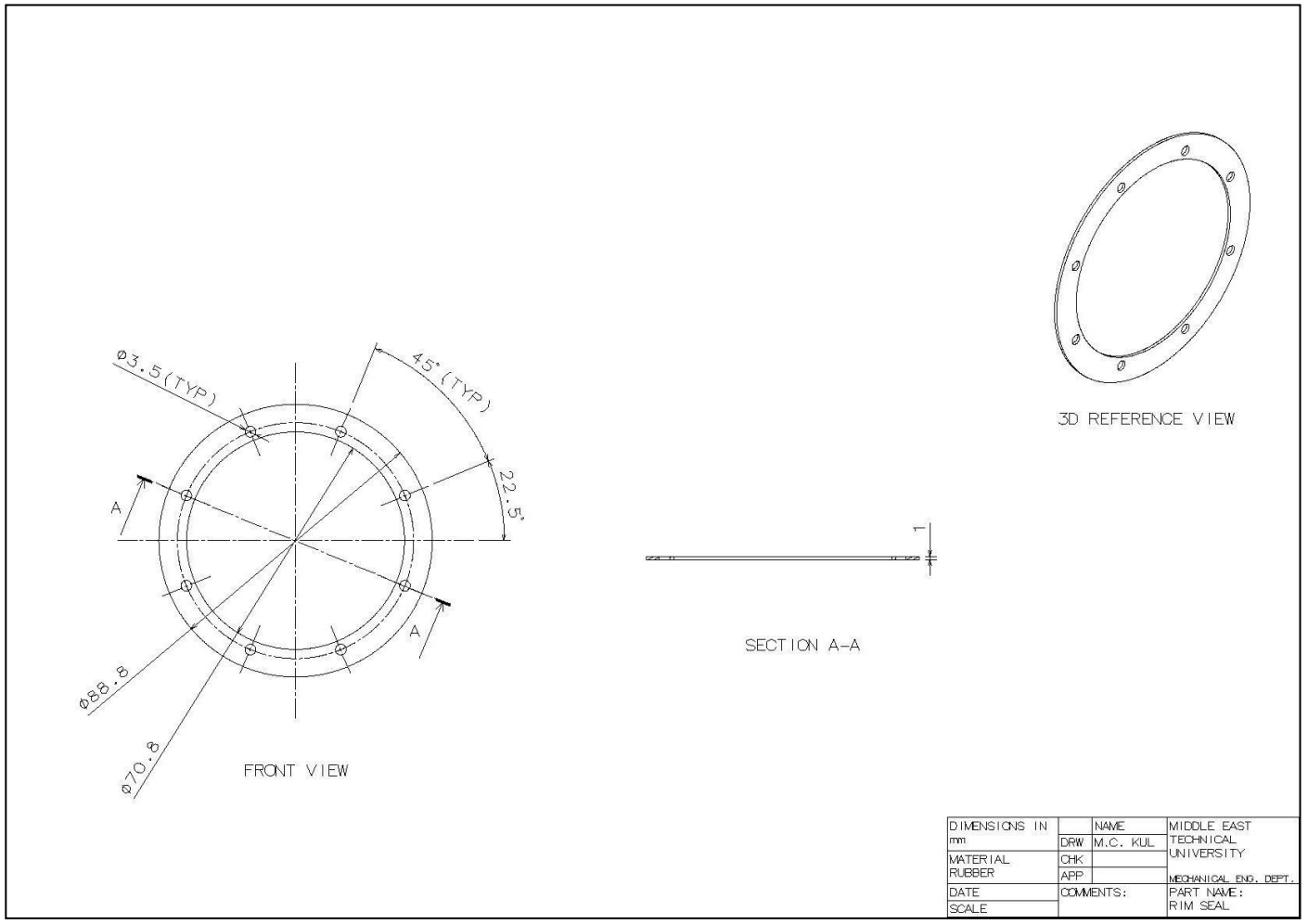

Figure 62 Rim seal technical drawing

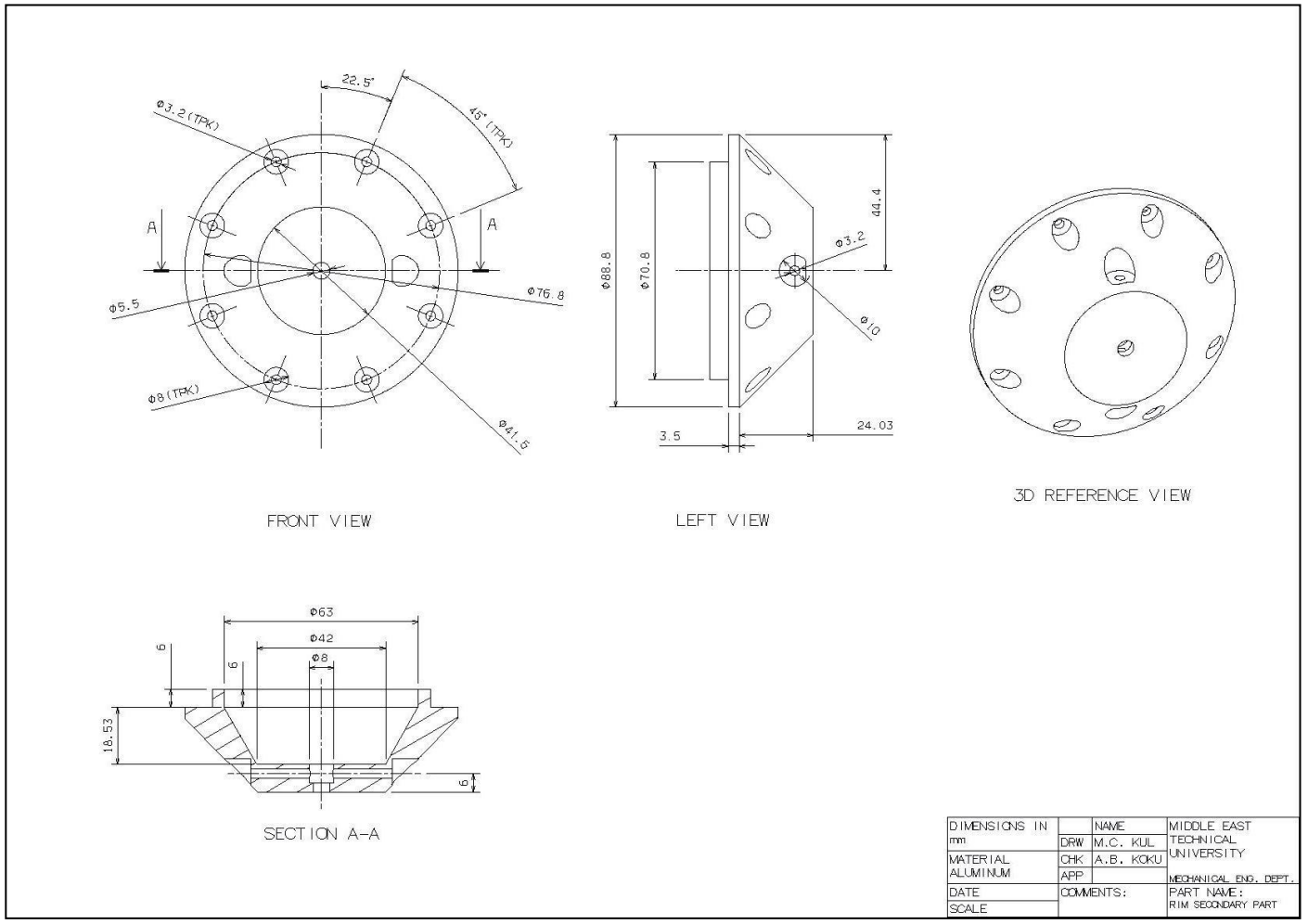

Figure 63 Rim secondary part technical drawing

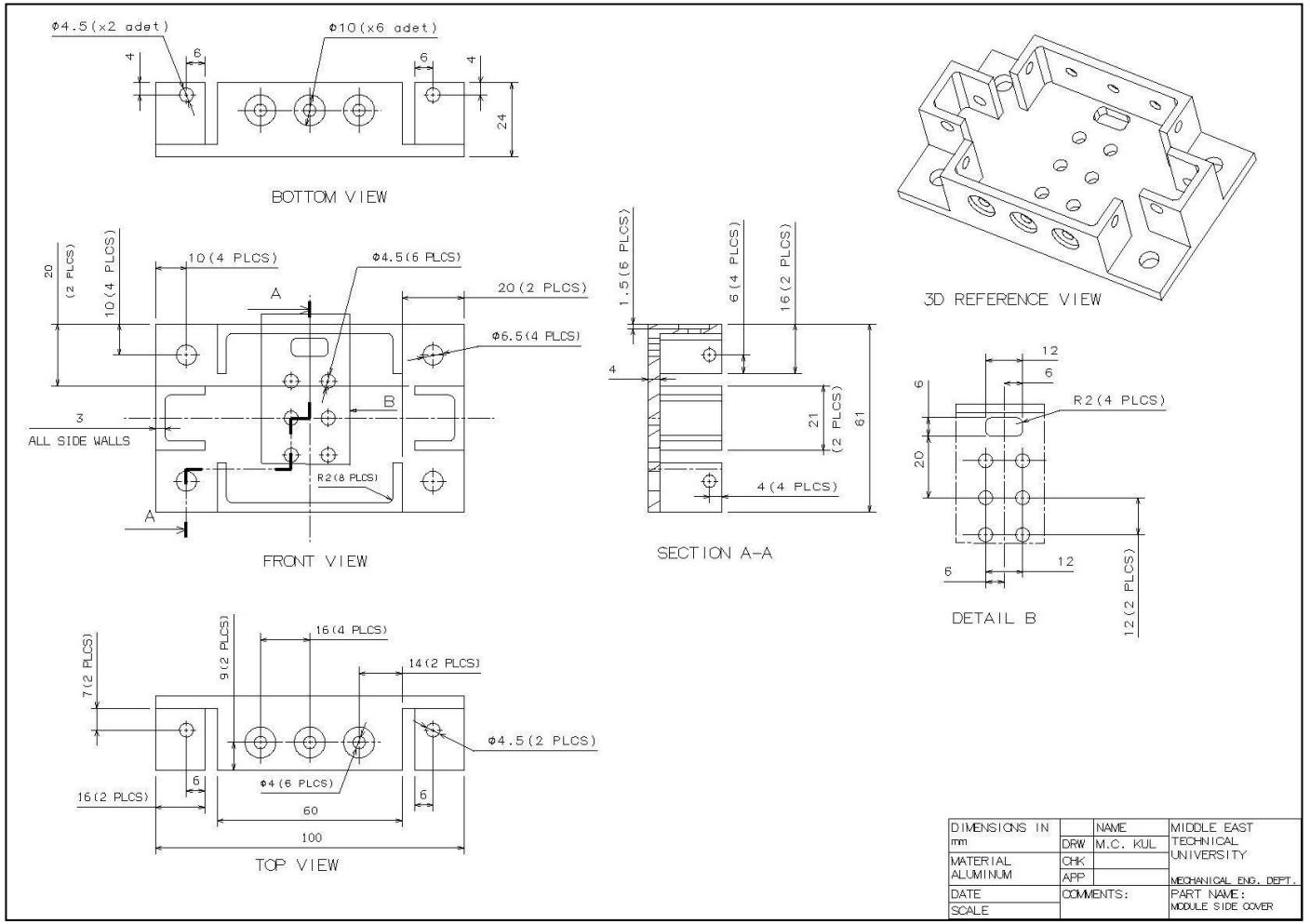

Figure 64 Module side cover technical drawing

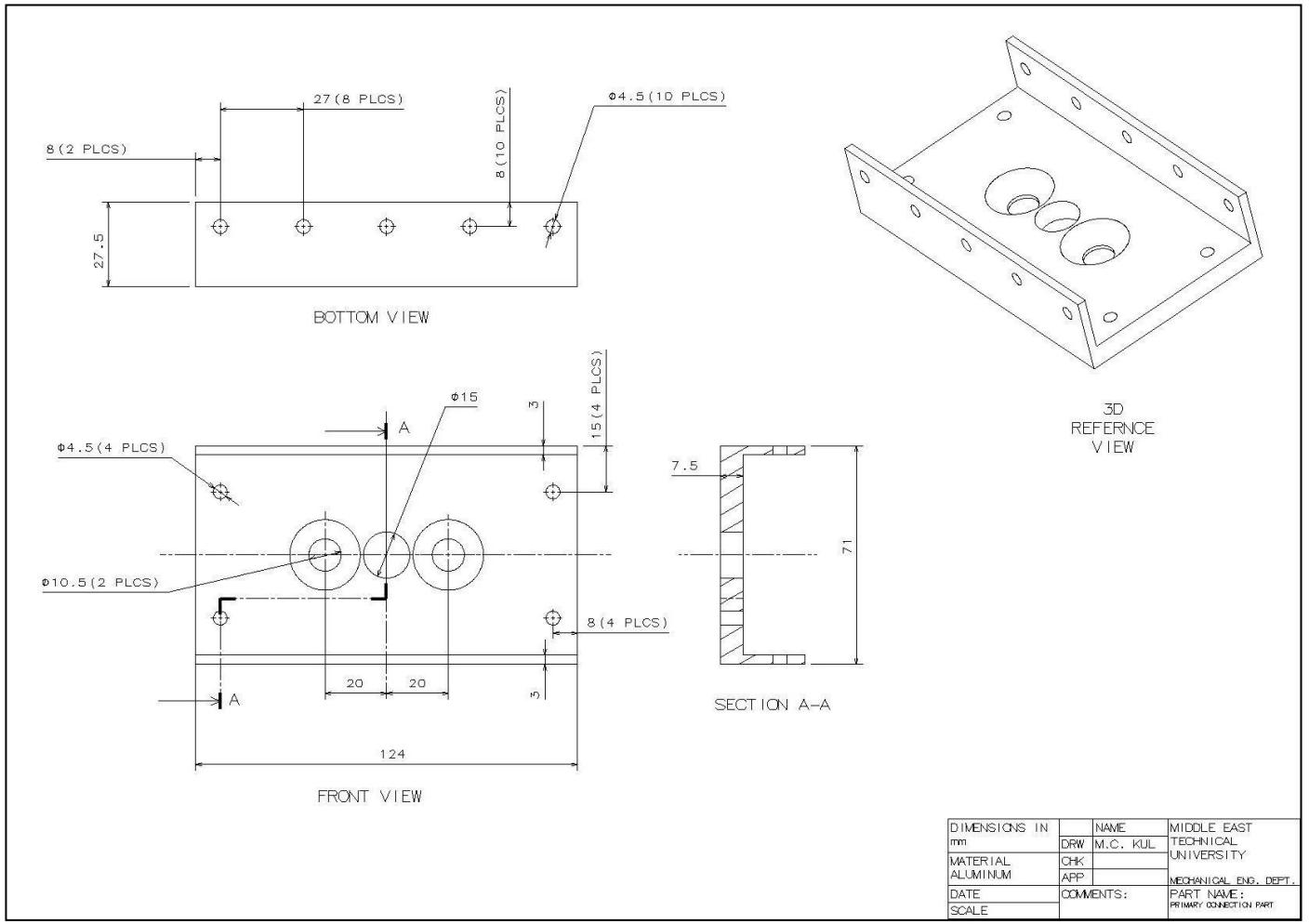

Figure 65 Primary connection part technical drawing

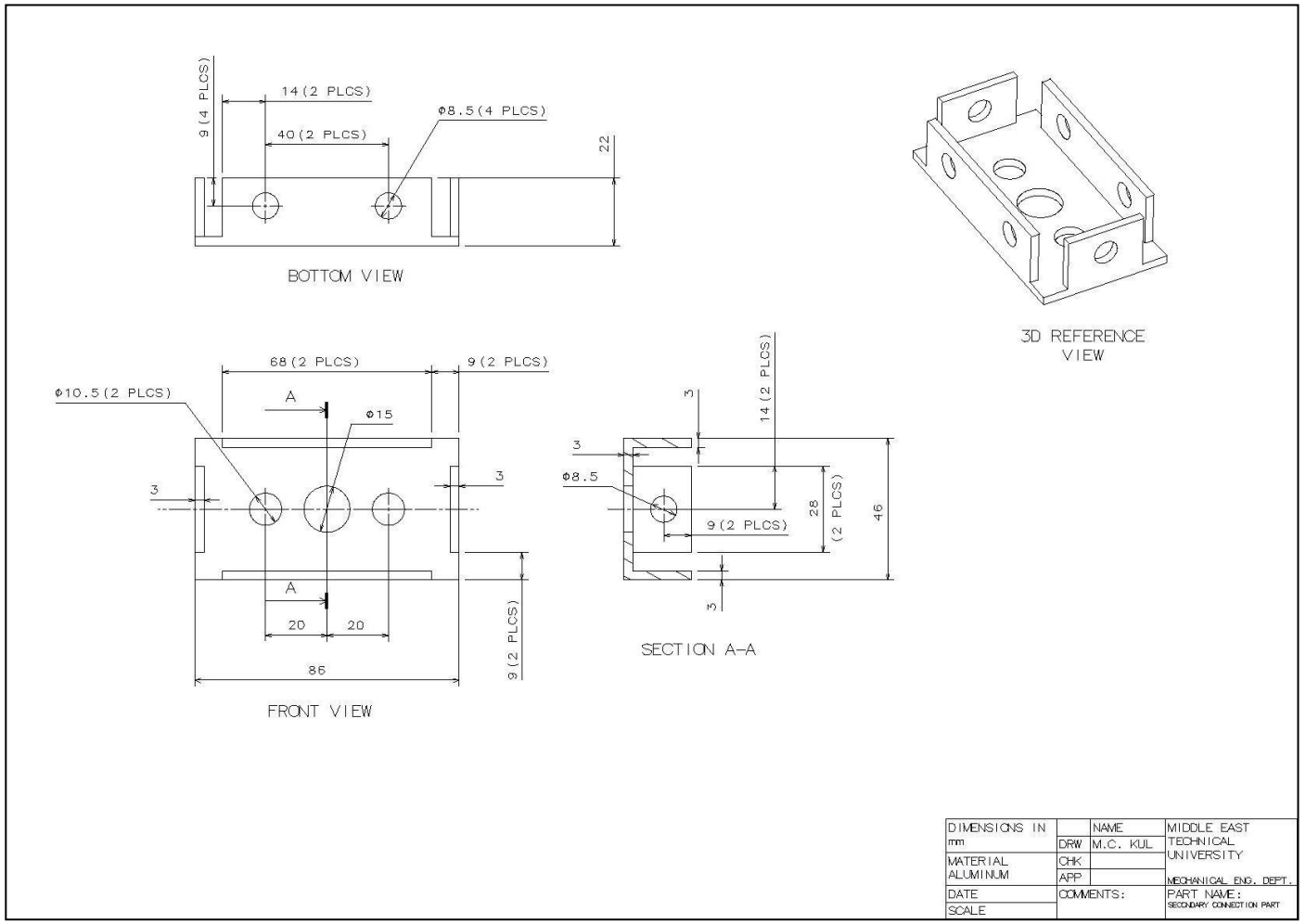

Figure 66 Secondary connection part technical drawing